

Patterns of nitrogen and phosphorus pools in terrestrial ecosystems in China

Yi-Wei Zhang^{1#}, Yanpei Guo^{1#}, Zhiyao Tang^{1*}, Yuhao Feng¹, Xinrong Zhu¹, Wenting Xu²,
Yongfei Bai², Guoyi Zhou³, Zongqiang Xie², Jingyun Fang¹

¹Institute of Ecology, College of Urban and Environmental Sciences and Key Laboratory for
Earth Surface Processes of the Ministry of Education, Peking University, Beijing 100871

²State Key Laboratory of Vegetation and Environmental Change, Institute of Botany, Chinese
Academy of Sciences, Beijing 100093

³Institute of Ecology, Jiangsu Key Laboratory of Agricultural Meteorology, Nanjing University
of Information Science & Technology, Nanjing 210044, China

[#]Equal contribution

Corresponding author:

Zhiyao Tang, Ph.D.

E-mail: zytang@urban.pku.edu.cn

Tel/Fax: +86-10-6275-4039

Abstract

Recent increases in atmospheric carbon dioxide (CO₂) and temperature relieve ~~the limitation~~
~~of these two~~their limitations on terrestrial ecosystem productivity, while nutrient availability
constrains the increasing plant photosynthesis more intensively. Nitrogen (N) and phosphorus
(P) are critical for plant physiological activities and consequently regulates ecosystem
productivity. Here, for the first time, we mapped N and P densities and concentrations of
leaves, woody stems, roots, litter and soil in forest, shrubland and grassland ecosystems
across China, based on an intensive investigation in 41754,865 sites, covering species
composition, biomass, and nutrient concentrations of different tissues of living plants, litter
and soil. Forest, shrubland and grassland ecosystems in China stored ~~7665.62 × 10⁶ Mg~~6803.6
Tg N, with ~~7434.53 × 10⁶ Mg~~(96.99~~6635.2 Tg N (97.5%)~~ fixed in soil (to a depth of one
metre), and ~~32.39 × 10⁶ Mg~~27.7 Tg N (0.42%), ~~59.4%),~~ ~~57 × 10⁶ Mg~~.8 Tg N (0.78%), ~~124.21~~
~~× 10⁶ Mg~~8%), 71.2 Tg N (1.62%) and ~~14.92 × 10⁶ Mg~~11.7 Tg N (0.192%) in leaves, stems,
roots and litter, respectively. The forest, shrubland and grassland ecosystems in China stored
~~3852.66 × 10⁶ Mg~~2806.0 Tg P, with ~~3821.64 × 10⁶ Mg~~2786.1 Tg P (99.493%) fixed in soil (to
a depth of one metre), and ~~3.36 × 10⁶ Mg (0.09%),~~ ~~14.06 × 10⁶ Mg~~2.7 Tg P (0.36%), ~~11.47 ×~~
~~10⁶ Mg~~1%), 9.4 Tg P (0.303%), 6.7 Tg P (0.2%) and ~~2.14 × 10⁶ Mg (0.06)~~1.0 Tg P (< 0.1%) in
leaves, stems, roots and litter, respectively. Our estimation showed that N pools were low in
northern China except Changbai Mountains, Mount Tianshan and Mount Alta, while
relatively higher values existed in eastern Qinghai-Tibetan Plateau and Yunnan. P densities in
~~plant organs~~vegetation were higher towards the south and ~~east~~northeast part of China, while
soil P density was higher towards the north and west part of China. The estimated N and P
density and concentrtaion datasets, “Patterns of nitrogen and phosphorus pools in terrestrial

ecosystems in China” (the pre-publication sharing link:
<https://datadryad.org/stash/share/78EBjhBqNoam2jOSoO1AXvbZtgIpCTi9eT-eGE7wyOk>),
are available from the Dryad Digital Repository (Zhang et al., 2020). These patterns of N and
P densities could potentially improve existing earth system models and large-scale researches
on ecosystem nutrients.

Key words: climate; nitrogen pools; phosphorus pools; nutrient limitation; spatial distribution

1 Introduction

Nitrogen (N) and phosphorus (P) play fundamental roles in plant physiological activities and functioning, such as photosynthesis, resource utilization and reproductive behaviours (Fernández-Martínez et al., 2019; Lovelock et al., 2004; Raaimakers et al., 1995), ultimately regulating plant growth and carbon (C) sequestration efficiency (Terrer et al., 2019); [Sun et al., 2017](#)). Under the background of global warming, the limiting factors for the plant growth, such as carbon dioxide (CO₂) and temperature, are becoming less restrictive for terrestrial ecosystem productivity (Norby et al., 2009; [Fatichi et al., 2019](#)), while nutrient availability tends to constrain the increasing plant photosynthesis more intensively (Cleveland et al., 2013; Du et al., 2020). As the key nutrients for plant growth, N and P independently or ~~together~~[jointly](#) limit biomass production (Elser et al., 2007; Finzi et al., 2007); [Hou et al., 2020](#)). N influence CO₂ assimilation in various ways (Vitousek and Howarth, 1991; [Campany et al., 2017](#)). For example, N is a critical element in chlorophyll (Field, 1983), and plant metabolic rates are also regulated by N content (Elser et al., 2010). P is crucial in RNA and DNA construction, and its content is associated with water uptake and transport (Carvajal et al., 1996; Cheeseman and Lovelock, 2004) as well as energy transfer and exchange (Achat et al., 2009). P shortage could lower photosynthetic C-assimilation rates (Lovelock et al., 2006).

In spite of the key importance of N and P for plants, knowledge on the patterns of their storage in terrestrial ecosystems are limited. With additional CO₂ entering atmosphere, more N could be ~~allotted~~[allocated](#) to plant growth and soil organic matter (SOM) accumulation, which may lead to less available mineral N for plant uptake (Luo et al., 2004). Direct and indirect evidences show that N limits productivity in temperate and boreal areas (Bonan, 1990; Miller, 1981; Vitousek, 1982). P originates from bedrock weathering and litter decomposition in

71 terrestrial ecosystems, and it experiences long-term biogeochemical processes before available
72 to plants (Föllmi, 1996), which consequently makes P a more predominant limiting factor to
73 ecosystem productivity (Reed et al., 2015). Additionally, P decomposition rates are constrained
74 by limited soil labile P storage, especially in tropical forests where soil P limitation is extreme
75 (Fisher et al., 2012).

76 Ecosystem models based on Amazon forest free air CO₂ enrichment (FACE) experiments
77 consistently showed that biomass C positively responded to simulated elevated CO₂, but the
78 models incorporating N and P availability showed lower plant growth than those not (Wieder
79 et al., 2015). Moreover, a recent study suggested that the inclusion of N and P availability into
80 the earth system models (ESMs) remarkably improved the estimation accuracy of C cycles over
81 previous models (Fleischer et al., 2019). Hence, understanding and predicting the patterns and
82 mechanisms of global C dynamics require well characterizing of N and P conditions.

83 N and P pools in ecosystems consist of several components that cast different influences
84 on ecosystem C storages and fluxes. For example, N and P in plants directly affect C
85 sequestration (Thomas et al., 2010), but their activities differ among organs (Elser et al., 2003;
86 Parks et al., 2000); the soil pools are the source of plant nutrition; and the litter pools act as a
87 transit link that returns nutrients from plants to soil (McGrath et al., 2000). Thus, an accurate
88 estimation of ecosystem N and P pools involves calculating specific nutrient densities in all
89 these components.

90 Terrestrial ecosystems in China play a considerable part in the continental and global C
91 cycles. Satellite data verified that China contributed to a 1/4 of global net increase in leaf area
92 from 2000 to 2017 (Chen et al., 2019). The total C pool in terrestrial ecosystems in China is
93 79.2 Pg C, and this number is still growing because of the nationwide ecological restoration

94 constructions, which accounted for 56% of the total C sequestration in the restoration area in
95 China from 2001 to 2010 (Lu et al., 2018). N and/or P limitations are ubiquitous in natural
96 ecosystems in China ([Augusto et al., 2017](#); [Du et al., 2020](#)); [Elser et al., 2007](#); [LeBauer and](#)
97 [Treseder, 2008](#); [Hou et al., 2020](#)). Understanding the distribution and allocation of N and P in
98 ecosystems is of great significance for a precise projection of C cycle in China. Although there
99 are a few studies on the spatial patterns of soil nutrient storages in China (Shangguan et al.,
100 2013; [Xu et al., 2020](#); Yang et al., 2007; Zhang et al., 2005), a thorough study on the distribution
101 of N and P pools of the whole ecosystems is still lacking, as vegetation (living or dead biomass)
102 composes the most active part of the nutrient stocks.

103 To fill this knowledge gap, here we identified N and P density patterns in China based on
104 an intensive field investigation, covering all components of the entire ecosystem, including
105 different plant organs, litter and soil. The present study aims to provide a high-resolution
106 ~~map~~maps of nutrient densities in different ecosystem components and to answer the following
107 questions.

108 1) How much N and P are stored in different components, i.e., leaf, stem, root, litter and
109 soil, of terrestrial ecosystems in China?

110 2) How do different components of N and P pools spatially distribute in China?

111 **2 Material and methods**

112 *2.1 Field sampling and nutrient density calculation*

113 Forest, shrublands and grasslands constitute major vegetation type groups in China.
114 Focusing primarily on these three groups, a nationwide, methodologically consistent field
115 investigation was conducted in June and September, 2011-2015.

116 In total, [41754865](#) sites, including [23853061](#) forest, [10691081](#) shrubland and [721723](#)

grassland sites, were investigated (Fig. S1a). At each site, one $20 \times 50 \text{ m}^2$ plot was set for forests, three replicated $5 \times 5 \text{ m}^2$ plots were set for shrublands, and ten $1 \times 1 \text{ m}^2$ plots were established for grasslands. Species composition and abundance were investigated in plots. Height (for trees, shrubs and herbs), diameter at breast height (DBH, at height 130 cm) (for trees), basal diameter (for shrubs) and crown width (for shrubs and herbs) were measured for all plant individuals in the plots (Tang et al., 2018a).

Leaves, stems (woody stems) and roots (without distinguishing coarse and fine roots) were sampled for the five top dominant tree and shrub species, and above- and belowground parts were sampled for dominant herb species. Soil was sampled to the depth of 1 m or to bedrock at the depths of 0–10, 10–20, 20–30, 30–50, and 50–100 cm with at least five replications per site to measure nutrient concentrations and bulk density after removing roots and gravels. Litter was sampled in at least three $1 \times 1 \text{ m}^2$ quadrats per site (for detailed survey protocol, see Tang et al., 2018a).

All samples were transported to laboratory, dried and measured. N concentrations of all samples were measured by a C/N analyzer (PE-2400 II; Perkin-Elmer, Boston, USA), while P concentrations were measured using the molybdate/ascorbic acid method after $\text{H}_2\text{SO}_4\text{-H}_2\text{O}_2$ digestion (Jones Jr, 2001). For the three organs, the community-level N or P density was the cumulative sum of the products of the corresponding biomass density (i.e. biomass per area, Mg ha^{-1}) and community-level concentrations for each co-occurring species. For detailed calculation of species biomass and community-level concentrations in each site, please referred to Tang et al (2018b).

$$N(P) = \sum_{\sum B_i \times \theta_i = 0}^n B_i \times \theta_i \quad (1)$$

$N(P)$ represents the community-level N or P density (Mg ha^{-1}); n is the total number

of plant species in one site; B_i is the biomass density of a specific organ of the i^{th} plant species in ~~onethat~~ site, where the plant organ biomass was estimated by allometric equations or harvesting; θ_i represents the N or P concentration (g kg^{-1}) of the same organ of the i^{th} plant species in that site. Allometric equation methods were adapted to trees and some shrubs (tree-like shrubs and xeric shrubs) for biomass estimation, while the biomass of grass-like shrubs and herbs were obtained by direct harvesting. Litter N or P density was litter biomass density (by harvesting) multiplied by litter N or P concentration of each sampling site. The soil N or P density was calculated to a depth of one metre. Soil N or P concentration and bulk density were measured at different depths (0–10, 10–20, 20–30, 30–50, and 50–100 cm) to determine the community-level soil N or P density using Equation (2):

$$\text{SOND(SOPD)} = \sum (1 - \delta_i) \times \rho_i \times C_i \times T_i / 10 \quad \text{SOND(SPD)} = \sum_{i=0}^n (1 - \delta_i) \times \rho_i \times C_i \times T_i / 10 \quad (2)$$

where ~~SOND(SOPD)~~, SOND(SPD) is the total N or P density of the soil within top 1 m (Mg ha^{-1}); n is the total number of soil layers (ranging from one to five) in the i^{th} layer (0–10, 10–20, 20–30, 30–50 and 50–100 cm), one site; δ_i is the volume percentage of gravel with a diameter > 2mm, ρ_i is the bulk density (g cm^{-3}), C_i is the soil N or P concentration (g kg^{-1}), and T_i is the depth (cm) of the i^{th} layer. For detailed calculations of species biomass and community-level concentrations at each site, please refer to previous studies (Tang et al., 2018a, ~~2018bb~~).

2.2 Climatic and vegetation data

The daily meteorological observation data from 2,400 meteorological stations across China were averaged over the 2011–2015 period to generate a spatial interpolation dataset of mean annual temperature (MAT) and precipitation (MAP), using a smooth spline function

(McVicar et al., 2007) , with a spatial resolution of 1 km. MAT and MAP of each site were extracted from this dataset.

Elevation was extracted from GTOPO30 with a spatial resolution of 30 arc-seconds (<http://edc.usgs.gov/products/elevation/gtopo30/gtopo30.html>). The mean enhanced vegetation index (EVI) from June to September during the 2011–2015 period was calculated based on MOD13A3 data with a resolution of 1 km (<https://modis.gsfc.nasa.gov/>).

The ranges of these variables of our field sites (EVI: 0.03~0.7; elevation: -137 m~5797 m; MAP: 19.8 mm~2316.3 mm; MAT: -5.2 °C~ 26.0 °C) could generally cover the ranges of corresponding variables in the focused vegetation types across China (99% ranges of EVI: 0.03~0.6; of elevation: 24 m~5628 m; of MAP: 50.6 mm~2956.5 mm; of MAT: -6.6 °C~22.8 °C).

Based on the level II vegetation classification of ChinaCover (Land Cover Atlas of the People's Republic of China Editorial Board, 2017), we classified the vegetation type groups into the following 13 ~~Vegetation~~vegetation types: five forest types, i.e., evergreen broadleaf forests, deciduous broadleaf forests, evergreen needle-leaf forests, deciduous needle-leaf forests, broadleaf and needle-leaf mixed forests; four shrubland types, i.e., evergreen broadleaf shrublands, deciduous broadleaf shrublands, evergreen needle-leaf shrublands, and sparse shrublands; and four grassland types, i.e., meadows, steppes, tussocks, and sparse grasslands.

2.3 Prediction the nationwide nutrient pools and distribution patterns

We used ~~back propagation artificial neural network for nutrient density spatial interpolating. The input layer contained~~random forest to predict the nutrient densities and

concentrations across China. The predictors included MAT, MAP, longitude, latitude, elevation, EVI and vegetation types (as dummy variables). We established one ~~artificial neural network~~ random forest model for N or P in each component (three plant organs, litter and ~~P in~~ five ~~components, soil layers~~), respectively. ~~The observation data~~ In each model, six variables were randomly ~~grouped into two subsets, 90% data for training~~ sampled at each split, and ~~the other 10% for~~ 500 trees were grown. Larger values of these parameters did not increase validation. ~~When building the artificial network, we used one and two layers, one to 20 hidden neurons per layer, respectively, to find out a model configuration with the best predicting ability. The training and testing process~~ R^2 obviously. Model prediction were repeated ~~100 times for each configuration. The best predicting model was selected according to the minimal mean root mean square error (RMSE). Then the chosen model was used to predict the nationwide nutrient distribution in corresponding component~~ for 100 times to obtain the average ~~conditions~~.

results. When modelling the nutrient densities in woody stems, we excluded the four grassland types. ~~The vegetation N or P density was the sum of all plant organs, and the ecosystem N or P density was the sum of all components.~~

All densities were log-transformed based on e , and explanatory variables were transformed using the following equation to ensure they were in the same range before modelling.

$$x'_i = \frac{x_i - \min(x)}{\max(x) - \min(x)} \quad (3)$$

where x_i means the i^{th} value of the environmental variables x , and $\max(x)$ and $\min(x)$ represent the maximum and minimum values of x , respectively. We estimated the relative importance of predictors using the increase in node purity for the splitting variable, which was measured by the reduction in residual sum of squares. The same procedures were repeated for

the prediction of N and P concentrations in different components across China. The spatial pattern of N:P ratio was calculated from the predicted N and P density datasets of the corresponding component.

The vegetation N or P density was the sum of all plant organs, the soil N or P density was the sum of all soil layers, and the ecosystem N or P density was the sum of all components. The soil depth data across China were obtained from Shangguan et al (2017). The N and P pools in 13 ~~Vegetation~~vegetation types were estimated, respectively. The N and P pools were calculated from the predicted nationwide densities. The predicted N and P densities were in 1 km spatial resolution, so the nutrient stock is the density multiply the grid area (1 km²) for each grid. The nutrient pools of a given vegetation type equals the sum of stocks of the grids belonging to that type.

2.4 ~~Data~~ Model validation and uncertainty ~~and validation~~

To evaluate the model performance, we calculated the linear relationship between the observed validation data (10% of the dataset by random sampling) and predicted data that was estimated based on training data (90% of the dataset by random sampling) for 100 times with the ~~selected~~ models for every component. ~~The~~We then calculated means of validation R^2 , slopes and intercepts of ~~these~~the 100 relationships ~~were estimated using standard major axis regression.~~ We also ~~mapped~~calculated the standard deviations (SDs) of the 100-time predictions of each component in each map grid to show the uncertainty of ~~our results in different regions~~the models.

All statistical analyses were performed using R 3.6.1 (R Core Team, 2019), ~~artificial~~ ~~networks~~random forests were built using ~~neuralnet~~randomForest package (GüntherLiauw and

Fritsch, 2010), and standard major axis regression was conducted using *smatr* package (Warton et al., 2012; Wiener, 2002).

3 Data accessibility

The datasets of N and P densities and concentration of different ecosystem components, "Patterns of nitrogen and phosphorus pools in terrestrial ecosystems in China", are available from the Dryad Digital Repository (the pre-publication sharing link: <https://datadryad.org/stash/share/78EBjhBqNoam2jOSoO1AXvbZtgIpCTi9eT-eGE7wyOk>) (Zhang et al., 2020).

4 Results

4.1 ~~Site average allocation~~ Allocation of nutrient ~~nutrients~~ among ecosystem components

The ~~site averaged mean~~ N and P densities varied among ~~forests, shrublands~~ forest, shrubland and ~~grasslands~~ grassland sites and among different tissues (Fig. 1 & 2) according to the measured ~~plot~~ data. ~~In On~~ average, leaves and woody stems in the forests stored more N than those in the shrublands (~~$11 \pm 100.1 \pm 0.1$ (mean \pm SD) $\times 10^{-2}$ Mg N ha⁻¹ vs. $34.2 \pm 10 \times 10^{-2}$ Mg N ha⁻¹ for leaves, and $260 \pm 340 \times 10^{-3} \pm 0.6$ Mg N ha⁻¹ vs. $5.8 \pm 111 \pm 20 \times 10^{-32}$ Mg N ha⁻¹ for woody stems).~~ Similarly, P densities were higher in the forests leaves and woody stems than those in the shrublands (~~$12 \pm 131.3 \pm 1.5 \times 10^{-32}$ Mg P ha⁻¹ vs. $2.9 \pm 3.1 \pm 6.15 \times 10^{-3}$ Mg P ha⁻¹ for leaves and $52 \pm 1105.6 \pm 11 \times 10^{-32}$ Mg P ha⁻¹ vs. $4.4 \pm 11.7 \pm 19 \times 10^{-3}$ Mg P ha⁻¹ for woody stems).~~ ~~than those in shrublands ($3.2 \pm 10 \times 10^{-2}$ Mg N ha⁻¹ and $2.9 \pm 6.1 \times 10^{-3}$ Mg P ha⁻¹ for leaves; $5.8 \pm 11 \times 10^{-3}$ Mg N ha⁻¹ and $4.4 \pm 11 \times 10^{-3}$ Mg P ha⁻¹ for woody stems) and grasslands ($2.7 \pm 2.4 \times 10^{-2}$ Mg N ha⁻¹ and $2.7 \pm 2.9 \times 10^{-3}$ Mg P ha⁻¹ for leaves).~~ However, the

root N and P densities in forests ($0.1 \pm 0.2 \text{ Mg N ha}^{-1}$ and $2.1 \pm 3 \times 10^{-1} \text{ Mg N ha}^{-1}$ and $1.8 \pm 2.8 \times 10^{-2} \text{ Mg P ha}^{-1}$) and grasslands ($1.9 \pm 1.7 \times 10^{-1} \text{ Mg N ha}^{-1}$ and $1.5 \pm 1.6 \times 10^{-2} \text{ Mg P ha}^{-1}$) were remarkably higher than in shrublands ($6.5 \pm 11 \times 10^{-2} \text{ Mg N ha}^{-1}$ and $6.1 \pm 9.9 \times 10^{-2} \text{ Mg N ha}^{-1}$ and $5.6 \pm 8.8 \times 10^{-3} \text{ Mg P ha}^{-1}$).

The site-averaged mean litter N densities ~~in forests, shrublands and grasslands~~ for forest, shrubland and grassland sites were $6.3 \pm 8.1 \pm 7.6 \times 10^{-2} \text{ Mg N ha}^{-1}$, $3.28 \pm 4.46 \times 10^{-2} \text{ Mg N ha}^{-1}$ and $5.5 \pm 9.3 \times 10^{-3} \text{ Mg N ha}^{-1}$, respectively. The site-averaged mean litter P densities in ~~forests, shrublands~~ forest, shrubland and ~~grasslands~~ grassland sites were $5.3 \pm 9.93 \times 10^{-3} \text{ Mg P ha}^{-1}$, $2.5 \pm 2 \pm 2.9.3 \times 10^{-3} \text{ Mg P ha}^{-1}$ and $4.141 \pm 7.1 \times 10^{-4} \text{ Mg P ha}^{-1}$, respectively.

The site-averaged mean soil N densities ~~in forests, shrublands and grasslands~~ for forest, shrubland and grassland sites were $11.2 \pm 9.212.1 \pm 10.8 \text{ Mg N ha}^{-1}$, $9.48.8 \pm 7.84 \text{ Mg N ha}^{-1}$ and $9.9 \pm 8.9 \text{ Mg N ha}^{-1}$, respectively. The site-averaged mean soil P densities were $4.9 \pm 6 \pm 4.2.5 \text{ Mg P ha}^{-1}$ in forest, $4.0 \pm \text{sites}$, 3.0 Mg P ha^{-1} in shrublands and $4.1 \pm 29 \pm 3.7 \text{ Mg P ha}^{-1}$ in ~~grasslands~~ shrubland sites and $4.4 \pm 2.8 \text{ Mg P ha}^{-1}$ in grassland sites.

~~Both belowground~~ Belowground vegetation N and P densities were higher than aboveground in grasslands and sparse shrublands ~~and grasslands~~. By contrast, this condition was reversed in forests and other 3 shrubland types (Fig. 3). Among various forest types, deciduous broadleaf forests and deciduous needle-leaf forests held the highest aboveground N and P densities, respectively. Evergreen needle-leaf forests held the lowest vegetation N density and evergreen broadleaf forests owned the lowest P density. For grassland types, ~~the density allocation varied markedly~~ Meadows and steppes meadows held higher N and P densities in belowground biomass than ~~tussocks and sparse grasslands~~ the other 3 grassland types, whereas these four grasslands types had relatively approximate nutrient densities in aboveground

biomass. Shrublands possessed the lowest vegetation N and P densities among three vegetation groups. Sparse shrublands owned the lowest vegetation nutrient densities and soil N density but the highest soil P density among four shrubland types.

4.2 Mapping of N and P densities in China's terrestrial ecosystems

All models of the N and P densities of different components performed well, with the validation R^2 ranging from 0.55 to 0.78 for plant organs and litter (Fig. 4), especially those for the woody stems ($R^2 = 0.81$ and 0.69 for N and P densities, respectively) from 0.47 to 0.62 for soil layers (Fig. 5). As to the concentration models, the validation R^2 varied from 0.45 to 0.63 for plant organs and litter ($R^2 = 0.66$ Fig. S2), and 0.62 for N and P densities, respectively) from 0.53 to 0.70 for soil layers (Fig. S3). Prediction results of 100-time repetitions were quite stable, as shown by SDs of N and P densities were relatively higher in western and northeastern China, with values > 5 (Fig. 5k-t). For example, the predictions of litter N (Fig. 5q) and P (Fig. 5r) showed larger SDs in western Xinjiang and Tibet close to zero in all components. (Fig S4 & S5).

The leaf N density was high in southern and eastern China, but low in northern and western China. It was especially high in the Changbai Mountains, the southern Tibet and the southeast coastal areas (Fig. 5), with a density $> 0.1 \text{ Mg N ha}^{-1}$. In comparison, China), while it was low in the northern Xinjiang and northern Inner Mongolia ($< 0.01 \text{ Mg N ha}^{-1}$). The woody stem and litter N densities showed the similar patterns to those of the leaves (Fig. 6c & g), whereas that in roots root N density was high in the Mount Tianshan, Mount Alta, Qinghai-Tibetan Plateau, northeastern mountainous area and the eastern Inner Mongolia steppe (Fig. 56e). The vegetation N density was relatively

300 ~~high~~higher in eastern China, ~~eastern~~ Qinghai-Tibetan Plateau, Mount Tianshan and Mount Alta,
301 ~~ranging from 0.5 to 2.5 Mg N ha⁻¹~~, (Fig. 7a). The soil and ecosystem N densities were low in
302 northern China except the Changbai Mountains, Mount Tianshan and Mount Alta, but high in
303 the eastern Qinghai-Tibetan Plateau and the Yunnan Province (Fig. 67c & e).

304 The P densities in leaves, woody stems, roots, ~~litter~~ and ~~litter~~the whole vegetation showed
305 similar patterns to the N densities in the corresponding components, respectively: (Fig. 6b, d, f
306 & h; Fig 7b). However, soil and ecosystem P densities were high in western and northern China
307 but low in eastern and southern China, ~~but low at high altitudes in the Qinghai-Tibetan Plateau~~
308 (Fig. 5 & 6 (Fig. 7d & f).

309 The N and P concentrations in plant organs and litter were generally higher in northern and
310 western mountain regions, but larger values of the former often occurs in northwestern part of
311 China, while those of the latter often occurs in northeastern part of China (Fig. S6a–h). The
312 spatial patterns of soil nutrient concentrations at different depths were consistent with those of
313 soil nutrient densities (Fig. S6i–r).

314 N:P ratio of plant organs and litter showed similar distribution patterns, higher values
315 occurring in southeastern and northwestern China and Qinghai-Tibetan Plateau (Fig. S7a–d).
316 Soil N:P ratio was higher in northeastern and southern China but lower in northwestern China
317 (Fig. S7e).

318 319 4.3 N and P pools in China's terrestrial ecosystems

320 In total, the terrestrial ecosystems in China stored ~~7665.62 × 10⁶ Mg~~6803.6 Tg N, with
321 ~~2632.80 × 10⁶ Mg~~2634.9 Tg N, ~~830.24 × 10⁶ Mg~~873.0 Tg N and ~~4202.58 × 10⁶ Mg~~3295.8 Tg
322 N stored in the forests, shrublands and grasslands, respectively (Table 1). Vegetation, litter and

soil stored 216.17×10^6 Mg 156.7 Tg N (2.82%), 14.92×10^6 Mg 3%), 11.7 Tg N (0.492%) and 7434.53×10^6 Mg 6635.2 Tg N (96.9997.5%), respectively. (Table 1).

China's terrestrial ecosystems stored 3852.66×10^6 Mg 2806.0 Tg P, with 1037.34×10^6 Mg 981.1 Tg P, 361.62×10^6 Mg 381.8 Tg P and 2453.70×10^6 Mg 1443.0 Tg P stored in the forest, shrublands and grasslands, respectively. Vegetation, litter and soil accounted for 28.88×10^6 Mg 18.8 Tg P (0.75%), 2.14×10^6 Mg 7%), 1.0 Tg P ($< 0.061\%$) and 3821.64×10^6 Mg 2786.1 Tg P (99.493%), respectively. (Table 1).

Meanwhile, N and P stocks among plant organs showed different allocation patterns (Table 2). Compared with the other two vegetation type groups, forests allocated the majority of N and P to the stem pool (59.29×10^6 Mg 55.5 Tg N and 13.81×10^6 Mg 9.2 Tg P), followed by the root pool (28.55×10^6 Mg 23.4 Tg N and 5.53×10^6 Mg 3.3 Tg P) and leaf pool (23.84×10^6 Mg 21.0 Tg N and 2.49×10^6 Mg 1 Tg P). However, the root pools in shrublands and grasslands held the most of N and P (4.44×10^6 Mg 3.8 Tg N and 0.38×10^6 Mg 3 Tg P for shrublands, and 91.22×10^6 Mg 71.2 Tg N and 5.55×10^6 Mg 6.7 Tg P for grasslands) (Table 2).

Among four grassland types, steppe had the largest N stock (1599.47×10^6 Mg 1370.1 Tg N), and sparse grasslands had the largest P stock (1578.83×10^6 Mg 507.2 Tg P) taking the ecosystem as a whole. Deciduous broadleaf shrublands owned the largest N and P stocks considering the whole ecosystem (605.09×10^6 Mg 577.6 Tg N and 211.15×10^6 Mg 234.2 Tg P) as well as in vegetation (5.30×10^6 Mg 5 Tg N and 0.58×10^6 Mg 5 Tg P), compared with the other 3 shrubland types. The largest ecosystem N and P stocks across all 13 vegetation five forest types appeared in evergreen needle-leaf forests (43.43×10^6 Mg 984.0 Tg N) and deciduous broadleaf forest (353.837×10^6 Mg Tg P) (Table 2).

5 Discussion

5.1 Performance ~~and uncertainty~~ of density models

The accuracy of the density models varied among different components. Soil interpolation models ~~Models for soil~~ showed ~~poorest~~ relatively poorer accuracy ($R^2=0.38$ ~~than models~~ for N plant organs and 0.27 for P) ~~among these models~~, litter (Fig. 4 & 5), partly because that soil N and P were ~~more stable than those in the plants and litters~~ (Matamala et al., 2008) and that soil ~~nutrient exchange and storage were~~ largely ~~controlled~~ influenced by ~~geochemical and geophysical processes~~ (geological conditions, soil age and parent material (Buol and Eswaran, 1999; Doetterl et al., 2015; Gray and Murphy, 2002), which ~~are were~~ not ~~considered~~ included in our ~~models~~ analysis because of the limited data availability. This can be evidenced by the decreasing validation R^2 of the models for soil N and P concentrations as well as N densities with soil depths (Fig. 5 and S3). The models preformed best for the stem N and P, because woody stems occupied the most biomass in the forest and shrublands (stem biomass/vegetation biomass were 0.68 and 0.48 for forest and shrublands, respectively). Climate variables could affect vegetation growth and biomass accumulation, and the variation in stem biomass could be the most direct reflection (~~Jozsa and Powell, 1987~~; Kirilenko and Sedjo, 2007; Jozsa and Powell, 1987; Poudel et al., 2011).

~~The predicted SDs were relatively higher in high latitudes and high altitudes, such as the northeastern mountainous area and the Qinghai Tibet Plateau, probably because of the lower sampling density. Meanwhile, the temperature in these regions was about the lower limit of the temperature range in our dataset, which could consequently lead to the weaker validity of the prediction results in such cold regions.~~

5.2 It is also noteworthy that the validation R^2 of the density models were higher than those of the concentration models for plant organs and litter (Fig. 4 & S2), which was opposite for soil layers (Fig. 5 and S3). They might reflect that biomass were more constrained by the selected factors in this study than nutrient concentrations in vegetation, while bulk density was less affected than nutrient concentrations in soil.

5.2 Nutrient pools in terrestrial ecosystems in China

Previous researches have estimated N and P stocks in soil across China. For example, Shangguan et al (2013) estimated that the storage of soil total N and P in the upper 1m of soil in China were 6.6 and 4.5 Pg. Yang et al (2007) estimated China's average density of soil N at a depth of one meter which was 0.84kg m^{-2} and the soil N stock was 7.4 Pg. Zhang et al (2005) investigated soil total P pool at a depth of 50 cm in China and concluded that the soil stock was 3.5 Pg with the total P density of soil $8.3 \times 10^2 \text{g/m}^3$. Our estimation of the soil N pool in China (6.6Pg) agreed with Shangguan et al (2013), but the estimated soil P pool (2.8Pg) was lower than the results of aforementioned studies. The mean soil N:P ratio in our study (2.5 of the predicted dataset and 2.1 of the training dataset) was lower than the result of Tian et al (2010), 5.2, while the spatial patterns in both studies are similar. Other than the researches focusing on soil, Xu et al (2020) estimated China's N storage by calculating the mean N densities of vegetation and soil from different ecoregions, and the reported that there were 10.43 Pg N in China's ecosystems, 10.14 Pg N in top 1 m soil and 0.29 Pg N in vegetation, both higher than our results (6.6 Pg N in soil and 0.16 Pg N in vegetation).

5.3 Potential driving factors of the N and P densities in various components

The distribution and allocation of N and P pools in ecosystems were largely determined by vegetation types and climate. The difference in the spatial patterns of nutrient pools could reflect the spatial variation in local vegetation. For example, it is obvious that the regions covered by forests tend to have higher ~~the~~ aboveground nutrient densities than those covered by other types, while the regions covered by sparse shrublands tend to have the lowest nutrient densities (Fig. 3). Despite its decisive influences on vegetation types, climate also impacts greatly on the nutrient utilization strategies of vegetation (Kirilenko and Sedjo, 2007; Poudel et al., 2011). For example, in southeastern China with higher precipitation and temperature, forests tend to allot more nutrient to organs related to growth, for example, leaves that perform photosynthesis and stems that related to resource transport and light competition (Zhang et al., 2018). These influences were reflected in our models (Fig. S8-S11). In the models of densities for plant organs and litter, vegetation types and climate variables showed higher relative importance. Heat and water are usually limited in the plateau and desert regions in western China, where shrublands and grasslands are dominant vegetation type groups. More nutrients are allocated to root systems by dominant plants in such stressful habitats to acquire resources from soil (Eziz et al., 2017; Kramer-Walter and Laughlin, 2017). ~~Soil nutrient densities were relatively larger~~Spatial variables, longitude and latitude, also held high importance, especially in the models for soil nutrients. On the one hand, it may result from their tight links with climate conditions. On the other hand, it may imply the influence of spatial correlation on nutrient pools. The effects of elevation and spatial variables were obvious from the prediction maps. There were relatively larger values of soil nutrient densities in the plateau and mountainous area in western China, possibly because of the lower rates of decomposition, mineralization, and nutrient ~~uptake~~input as well as less leaching loss in high-altitude regions (Bonito et al., 2003;

Vincent et al., 2014). However, the distribution patterns of soil nutrient densities in eastern China were generally consistent with the Soil Substrate Age hypothesis that the younger and less-leached soil in temperate regions tend to be more N limited but less P limited than the elder and more-leached soil in tropical and subtropical regions (Reich and Oleksyn, 2004; Vitousek et al., 2010; Walker and Syers, 1976). Additionally, such patterns reflect that the factors not investigated in this study, such as soil age and parent material, could contribute to the patterns of nutrient pools, which should be considered in future researches as potential drivers (Augusto et al., 2017; Porder and Chadwick, 2009).

5.3.4 Potential applications of the data

Atmospheric CO₂ enrichment trend was undoubtable, but how this procedure will develop is still unclear (Fatichi et al., 2019). A number of previous studies proved that global carbon cycle models would produce remarkable bias if overlooking the coupled nutrient cycle (Fleischer et al., 2019; Hungate et al., 2003; Thornton et al., 2007). However, high-resolution and accurate ecosystem nutrient datasets were unattainable and hard to be modeled without enormous field investigation basis. This study relied on nationwide field survey data, providing comprehensive N and P density datasets of different ecosystem components. Based on the present dataset, enhancement could be made in various ecosystem research aspects.

First and foremost, the dataset could facilitate the improvement in the prediction of large-scale terrestrial C budget, thereby to better understand patterns and mechanisms of C cycle as well as the future trend of climate change (Le Quéré et al., 2018). Numerous projections of future C sequestration overestimated the amount of C fixed by vegetation due to the neglect of nutrient limitation (Cooper et al., 2002; Cramer et al., 2001). Global C cycling models coupled

with nutrient cycle ~~could~~[may](#) make more accurate predictions of carbon dynamics. Moreover, our dataset illustrated N and P densities of major ecosystem components and vegetation types at a high spatial resolution for the first time, which could help identify C and nutrient allocation patterns from the tissue level to the community level, especially for vegetation organs which still lack large-scale nutrient datasets.

In addition, large-scale N and P pool spatial patterns could provide the data references for the vegetation researches using remote sensing (Jetz et al., 2016). Vegetation nutrient densities was important traits but hard to be extracted and detected remotely. With the development of hyperspectral remote sensing technology and theory of spectral diversity, foliar nutrient traits can be successfully predicted (Skidmore et al., 2010; Wang et al., 2019). However, previous studies still focused on finer-scale patterns and were constrained by the lack of large-scale field datasets for uncertainties assessment (Singh et al., 2015). Our nationwide nutrient dataset offers an opportunity to enlarge the generality of remote-sensing models and algorithms at large scales.

Funding

This work was funded by the National Key Research and Development Project (2019YFA0606602), the National Natural Science Foundation of China (32025025, 31770489, 31988102) and the Strategic Priority Research Programme of the Chinese Academy of Sciences (XDA27010102, XDA05050000).—

Author Contributions

Z.T. designed the research. Y.W.Z, Y.G., Y.F., and X.Z. analysed the data. W.X., Y.B., G.Z., Z.X. and Z.T. organized the field investigation. Y.W.Z, Y.G., Z.T. wrote the manuscript and all authors contributed substantially to revisions.

461

462 **Competing interests**

463 The authors declare no competing interests.

464

Reference

- Achat, D. L., Bakker, M. R., and Morel, C.: Process-based assessment of phosphorus availability in a low phosphorus sorbing forest soil using isotopic dilution methods., *Soil Sci. Soc. Am. J.*, 73, 2131–2142, 2009.
- Augusto, L., Achat, D. L., Jonard, M., Vidal, D., and Ringeval, B.: Soil parent material-A major driver of plant nutrient limitations in terrestrial ecosystems, *Glob Chang Biol*, 23, 3808–3824, <https://doi.org/10.1111/gcb.13691>, 2017.
- Bonan, G. B.: Carbon and nitrogen cycling in North American boreal forests, *Biogeochemistry*, 10, 1–28, <https://doi.org/10.1007/BF00000889>, 1990.
- Bonito, G. M., Coleman, D. C., Haines, B. L., and Cabrera, M. L.: Can nitrogen budgets explain differences in soil nitrogen mineralization rates of forest stands along an elevation gradient?, *Forest Ecology and Management*, 176, 563–574, [https://doi.org/10.1016/S0378-1127\(02\)00234-7](https://doi.org/10.1016/S0378-1127(02)00234-7), 2003.
- Buol, S. W. and Eswaran, H.: Oxisols, in: *Advances in Agronomy*, vol. 68, edited by: Sparks, D. L., Academic Press, 151–195, [https://doi.org/10.1016/S0065-2113\(08\)60845-7](https://doi.org/10.1016/S0065-2113(08)60845-7), 1999.
- Campany, C. E., Medlyn, B. E., and Duursma, R. A.: Reduced growth due to belowground sink limitation is not fully explained by reduced photosynthesis, *Tree Physiol*, 37, 1042–1054, <https://doi.org/10.1093/treephys/tpx038>, 2017.
- Carvajal, M., Cooke, D. T., and Clarkson, D. T.: Responses of wheat plants to nutrient deprivation may involve the regulation of water-channel function, *Planta*, 199, 372–381, <https://doi.org/10.1007/BF00195729>, 1996.
- Cheeseman, J. M. and Lovelock, C. E.: Photosynthetic characteristics of dwarf and fringe *Rhizophora mangle* L. in a Belizean mangrove, *Plant Cell Environ.*, 27, 769–780, <https://doi.org/10.1111/j.1365-3040.2004.01181.x>, 2004.
- Chen, C., Park, T., Wang, X., Piao, S., Xu, B., Chaturvedi, R. K., Fuchs, R., Brovkin, V., Ciais, P., Fensholt, R., Tømmervik, H., Bala, G., Zhu, Z., Nemani, R. R., and Myneni, R. B.: China and India lead in greening of the world through land-use management, *Nat. Sustain.*, 2, 122–129, <https://doi.org/10.1038/s41893-019-0220-7>, 2019.

492 Cleveland, C. C., Houlton, B. Z., Smith, W. K., Marklein, A. R., Reed, S. C., Parton, W., Grosso, S.
 493 J. D., and Running, S. W.: Patterns of new versus recycled primary production in the terrestrial
 494 biosphere, *Proc. Natl. Acad. Sci. U. S. A.*, 110, 12733–12737,
 495 <https://doi.org/10.1073/pnas.1302768110>, 2013.

496 Cooper, R. N., Houghton, J. T., McCarthy, J. J., and Metz, B.: *Climate Change 2001: The Scientific*
 497 *Basis*, Cambridge University Press, Cambridge, UK, 2002.

498 Cramer, W., Bondeau, A., Woodward, F. I., Prentice, I. C., Betts, R. A., Brovkin, V., Cox, P. M.,
 499 Fisher, V., Foley, J. A., Friend, A. D., Kucharik, C., Lomas, M. R., Ramankutty, N., Sitch, S., Smith,
 500 B., White, A., and Young-Molling, C.: Global response of terrestrial ecosystem structure and
 501 function to CO₂ and climate change: results from six dynamic global vegetation models, *Glob.*
 502 *Change Biol.*, 7, 357–373, <https://doi.org/10.1046/j.1365-2486.2001.00383.x>, 2001.

503 Doetterl, S., Stevens, A., Six, J., Merckx, R., Van Oost, K., Casanova Pinto, M., Casanova-Katny,
 504 A., Muñoz, C., Boudin, M., Zagal Venegas, E., and Boeckx, P.: Soil carbon storage controlled by
 505 interactions between geochemistry and climate, *Nat. Geosci.*, 8, 780–783,
 506 <https://doi.org/10.1038/ngeo2516>, 2015.

507 Du, E., Terrer, C., Pellegrini, A. F. A., Ahlström, A., van Lissa, C. J., Zhao, X., Xia, N., Wu, X., and
 508 Jackson, R. B.: Global patterns of terrestrial nitrogen and phosphorus limitation, 13, 221–226,
 509 <https://doi.org/10.1038/s41561-019-0530-4>, 2020.

510 Elser, J. J., Acharya, K., Kyle, M., Cotner, J., Makino, W., Markow, T., Watts, T., Hobbie, S., Fagan,
 511 W., Schade, J., Hood, J., and Sterner, R. W.: Growth rate–stoichiometry couplings in diverse biota,
 512 *Ecol. Lett.*, 6, 936–943, <https://doi.org/10.1046/j.1461-0248.2003.00518.x>, 2003.

513 Elser, J. J., Bracken, M. E. S., Cleland, E. E., Gruner, D. S., Harpole, W. S., Hillebrand, H., Ngai, J.
 514 T., Seabloom, E. W., Shurin, J. B., and Smith, J. E.: Global analysis of nitrogen and phosphorus
 515 limitation of primary producers in freshwater, marine and terrestrial ecosystems, *Ecol. Lett.*, 10,
 516 1135–1142, <https://doi.org/10.1111/j.1461-0248.2007.01113.x>, 2007.

517 Elser, J. J., Fagan, W. F., Kerkhoff, A. J., Swenson, N. G., and Enquist, B. J.: Biological
 518 stoichiometry of plant production: metabolism, scaling and ecological response to global change:
 519 *Tansley review*, 186, 593–608, <https://doi.org/10.1111/j.1469-8137.2010.03214.x>, 2010.

520 Fatichi, S., Pappas, C., Zscheischler, J., and Leuzinger, S.: Modelling carbon sources and sinks in
521 terrestrial vegetation, *New Phytol.*, 221, 652–668, <https://doi.org/10.1111/nph.15451>, 2019.

522 Fernández-Martínez, M., Pearse, I., Sardans, J., Sayol, F., Koenig, W. D., LaMontagne, J. M.,
523 Bogdziewicz, M., Collalti, A., Hacket-Pain, A., Vacchiano, G., Espelta, J. M., Peñuelas, J., and
524 Janssens, I. A.: Nutrient scarcity as a selective pressure for mast seeding, *Nat. Plants*, 5, 1222–1228,
525 <https://doi.org/10.1038/s41477-019-0549-y>, 2019.

526 Field, C.: Allocating leaf nitrogen for the maximization of carbon gain: Leaf age as a control on the
527 allocation program, *Oecologia*, 56, 341–347, <https://doi.org/10.1007/BF00379710>, 1983.

528 Finzi, A. C., Norby, R. J., Calfapietra, C., Gallet-Budynek, A., Gielen, B., Holmes, W. E., Hoosbeek,
529 M. R., Iversen, C. M., Jackson, R. B., Kubiske, M. E., Ledford, J., Liberloo, M., Oren, R., Polle, A.,
530 Pritchard, S., Zak, D. R., Schlesinger, W. H., and Ceulemans, R.: Increases in nitrogen uptake rather
531 than nitrogen-use efficiency support higher rates of temperate forest productivity under elevated
532 CO₂, *Proc. Natl. Acad. Sci. U. S. A.*, 104, 14014–14019, <https://doi.org/10.1073/pnas.0706518104>,
533 2007.

534 Fisher, J. B., Badgley, G., and Blyth, E.: Global nutrient limitation in terrestrial vegetation, *Glob.*
535 *Biogeochem. Cycle*, 26, GB3007, <https://doi.org/10.1029/2011GB004252>, 2012.

536 Fleischer, K., Rammig, A., De Kauwe, M. G., Walker, A. P., Domingues, T. F., Fuchslueger, L.,
537 Garcia, S., Goll, D. S., Grandis, A., Jiang, M., Haverd, V., Hofhansl, F., Holm, J. A., Kruijt, B.,
538 Leung, F., Medlyn, B. E., Mercado, L. M., Norby, R. J., Pak, B., von Randow, C., Quesada, C. A.,
539 Schaap, K. J., Valverde-Barrantes, O. J., Wang, Y.-P., Yang, X., Zaehle, S., Zhu, Q., and Lapola, D.
540 M.: Amazon forest response to CO₂ fertilization dependent on plant phosphorus acquisition, *Nat.*
541 *Geosci.*, 12, 736–741, <https://doi.org/10.1038/s41561-019-0404-9>, 2019.

542 Föllmi, K. B.: The phosphorus cycle, phosphogenesis and marine phosphate-rich deposits, *Earth-*
543 *Sci. Rev.*, 40, 55–124, [https://doi.org/10.1016/0012-8252\(95\)00049-6](https://doi.org/10.1016/0012-8252(95)00049-6), 1996.

544 Gray, J. and Murphy, B. W.: Parent material and world soil distribution, 14, 2002.

545 Hou, E., Luo, Y., Kuang, Y., Chen, C., Lu, X., Jiang, L., Luo, X., and Wen, D.: Global meta-analysis
546 shows pervasive phosphorus limitation of aboveground plant production in natural terrestrial
547 ecosystems, *Nat Commun*, 11, 637, <https://doi.org/10.1038/s41467-020-14492-w>, 2020.

548 Hungate, B. A., Dukes, J. S., Shaw, M. R., Luo, Y., and Field, C. B.: Nitrogen and Climate Change,
549 Science, 302, 1512–1513, <https://doi.org/10.1126/science.1091390>, 2003.

550 Jetz, W., Cavender-Bares, J., Pavlick, R., Schimel, D., Davis, F. W., Asner, G. P., Guralnick, R.,
551 Kattge, J., Latimer, A. M., Moorcroft, P., Schaepman, M. E., Schildhauer, M. P., Schneider, F. D.,
552 Schrod, F., Stahl, U., and Ustin, S. L.: Monitoring plant functional diversity from space, Nat. Plants,
553 2, 16024, <https://doi.org/10.1038/nplants.2016.24>, 2016.

554 Jones Jr, J. B.: Laboratory guide for conducting soil tests and plant analysis, CRC press, New York,
555 2001.

556 Jozsa, L. A. and Powell, J. M.: Some climatic aspects of biomass productivity of white spruce stem
557 wood, 17, 1075–1079, <https://doi.org/10.1139/x87-165>, 1987.

558 Kirilenko, A. P. and Sedjo, R. A.: Climate change impacts on forestry, Proc. Natl. Acad. Sci. U. S.
559 A., 104, 19697–19702, <https://doi.org/10.1073/pnas.0701424104>, 2007.

560 Land Cover Atlas of the People’s Republic of China Editorial Board: Land Cover Atlas of the
561 People’s Republic of China (1:1000000), China Map Publishing House, Beijing, 2017.

562 Le Quéré, C., Andrew, R. M., Friedlingstein, P., Sitch, S., Pongratz, J., Manning, A. C., Korsbakken,
563 J. I., Peters, G. P., Canadell, J. G., Jackson, R. B., Boden, T. A., Tans, P. P., Andrews, O. D., Arora,
564 V. K., Bakker, D. C. E., Barbero, L., Becker, M., Betts, R. A., Bopp, L., Chevallier, F., Chini, L. P.,
565 Ciais, P., Cosca, C. E., Cross, J., Currie, K., Gasser, T., Harris, I., Hauck, J., Haverd, V., Houghton,
566 R. A., Hunt, C. W., Hurtt, G., Ilyina, T., Jain, A. K., Kato, E., Kautz, M., Keeling, R. F., Klein
567 Goldewijk, K., Körtzinger, A., Landschützer, P., Lefèvre, N., Lenton, A., Lienert, S., Lima, I.,
568 Lombardozzi, D., Metzl, N., Millero, F., Monteiro, P. M. S., Munro, D. R., Nabel, J. E. M. S.,
569 Nakaoka, S., Nojiri, Y., Padin, X. A., Peregon, A., Pfeil, B., Pierrot, D., Poulter, B., Rehder, G.,
570 Reimer, J., Rödenbeck, C., Schwinger, J., Séférian, R., Skjelvan, I., Stocker, B. D., Tian, H.,
571 Tilbrook, B., Tubiello, F. N., van der Laan-Luijkx, I. T., van der Werf, G. R., van Heuven, S., Viovy,
572 N., Vuichard, N., Walker, A. P., Watson, A. J., Wiltshire, A. J., Zaehle, S., and Zhu, D.: Global carbon
573 budget 2017, Earth Syst. Sci. Data, 10, 405–448, <https://doi.org/10.5194/essd-10-405-2018>, 2018.

574 LeBauer, D. S. and Treseder, K. K.: Nitrogen limitation of net primary productivity in terrestrial
575 ecosystems is globally distributed, Ecology, 89, 371–379, <https://doi.org/10.1890/06-2057.1>, 2008.

576 Liaw, A. and Wiener, M.: Classification and regression by randomForest, 2, 18–22, 2002.

577 Lovelock, C. E., Feller, I. C., Mckee, K. L., Engelbrecht, B. M. J., and Ball, M. C.: The effect of
 578 nutrient enrichment on growth, photosynthesis and hydraulic conductance of dwarf mangroves in
 579 Panama, *Funct Ecology*, 18, 25–33, <https://doi.org/10.1046/j.0269-8463.2004.00805.x>, 2004.

580 Lovelock, C. E., Feller, I. C., Ball, M. C., Engelbrecht, B. M. J., and Ewe, M. L.: Differences in
 581 plant function in phosphorus- and nitrogen-limited mangrove ecosystems, *New Phytol.*, 172, 514–
 582 522, <https://doi.org/10.1111/j.1469-8137.2006.01851.x>, 2006.

583 Lu, F., Hu, H., Sun, W., Zhu, J., Liu, G., Zhou, W., Zhang, Q., Shi, P., Liu, X., Wu, X., Zhang, L.,
 584 Wei, X., Dai, L., Zhang, K., Sun, Y., Xue, S., Zhang, W., Xiong, D., Deng, L., Liu, B., Zhou, L.,
 585 Zhang, C., Zheng, X., Cao, J., Huang, Y., He, N., Zhou, G., Bai, Y., Xie, Z., Tang, Z., Wu, B., Fang,
 586 J., Liu, G., and Yu, G.: Effects of national ecological restoration projects on carbon sequestration in
 587 China from 2001 to 2010, *Proc. Natl. Acad. Sci. U. S. A.*, 115, 4039–4044,
 588 <https://doi.org/10.1073/pnas.1700294115>, 2018.

589 Luo, Y., Su, B., Currie, W. S., Dukes, J. S., Finzi, A., Hartwig, U., Hungate, B., McMurtrie, R. E.,
 590 Oren, R., Parton, W. J., Pataki, D. E., Shaw, R. M., Zak, D. R., and Field, C. B.: Progressive Nitrogen
 591 Limitation of Ecosystem Responses to Rising Atmospheric Carbon Dioxide, *BioScience*, 54, 731–
 592 739, [https://doi.org/10.1641/0006-3568\(2004\)054\[0731:PNLOER\]2.0.CO;2](https://doi.org/10.1641/0006-3568(2004)054[0731:PNLOER]2.0.CO;2), 2004.

593 McGrath, D. A., Comerford, N. B., and Duryea, M. L.: Litter dynamics and monthly fluctuations in
 594 soil phosphorus availability in an Amazonian agroforest, *For. Ecol. Manage.*, 131, 167–181,
 595 [https://doi.org/10.1016/S0378-1127\(99\)00207-8](https://doi.org/10.1016/S0378-1127(99)00207-8), 2000.

596 McVicar, T. R., Van Niel, T. G., Li, L., Hutchinson, M. F., Mu, X., and Liu, Z.: Spatially distributing
 597 monthly reference evapotranspiration and pan evaporation considering topographic influences,
 598 *Journal of Hydrology*, 338, 196–220, <https://doi.org/10.1016/j.jhydrol.2007.02.018>, 2007.

599 Miller, H. G.: Forest Fertilization: Some Guiding Concepts, *Forestry*, 54, 157–167,
 600 <https://doi.org/10.1093/forestry/54.2.157>, 1981.

601 Norby, R. J., Warren, J. M., Iversen, C. M., Garten, C. T., Medlyn, B. E., and McMurtrie, R. E.: 1
 602 CO₂ Enhancement of Forest Productivity Constrained by 2 Limited Nitrogen Availability, 15, 2009.

603 Parks, S. E., Haigh, A. M., and Cresswell, G. C.: Stem tissue phosphorus as an index of the
 604 phosphorus status of *Banksia ericifolia* L. f., *Plant Soil*, 227, 59–65,
 605 <https://doi.org/10.1023/A:1026563926187>, 2000.

606 Porder, S. and Chadwick, O. A.: Climate and soil-age constraints on nutrient uplift and retention by
 607 plants, *Ecology*, 90, 623–636, <https://doi.org/10.1890/07-1739.1>, 2009.

608 Poudel, B. C., Sathre, R., Gustavsson, L., Bergh, J., Lundström, A., and Hyvönen, R.: Effects of
 609 climate change on biomass production and substitution in north-central Sweden, *Biomass and*
 610 *Bioenergy*, 35, 4340–4355, <https://doi.org/10.1016/j.biombioe.2011.08.005>, 2011.

611 Quinn Thomas, R., Canham, C. D., Weathers, K. C., and Goodale, C. L.: Increased tree carbon
 612 storage in response to nitrogen deposition in the US, *Nat. Geosci.*, 3, 13–17,
 613 <https://doi.org/10.1038/ngeo721>, 2010.

614 R Core Team: R: A language and environment for statistical computing, Vienna, 2019.

615 Raaimakers, D., Boot, R. G. A., Dijkstra, P., Pot, S., and Pons, T.: Photosynthetic Rates in Relation
 616 to Leaf Phosphorus Content in Pioneer versus Climax Tropical Rainforest Trees, 102, 120–125,
 617 1995.

618 Reed, S. C., Yang, X., and Thornton, P. E.: Incorporating phosphorus cycling into global modeling
 619 efforts: a worthwhile, tractable endeavor, *New Phytol.*, 208, 324–329,
 620 <https://doi.org/10.1111/nph.13521>, 2015.

621 Reich, P. B. and Oleksyn, J.: Global patterns of plant leaf N and P in relation to temperature and
 622 latitude, *Proc. Natl. Acad. Sci. U. S. A.*, 101, 11001–11006,
 623 <https://doi.org/10.1073/pnas.0403588101>, 2004.

624 Shangguan, W., Dai, Y., Liu, B., Zhu, A., Duan, Q., Wu, L., Ji, D., Ye, A., Yuan, H., Zhang, Q., Chen,
 625 D., Chen, M., Chu, J., Dou, Y., Guo, J., Li, H., Li, J., Liang, L., Liang, X., Liu, H., Liu, S., Miao,
 626 C., and Zhang, Y.: A China data set of soil properties for land surface modeling, *J. Adv. Model. Earth*
 627 *Syst.*, 5, 212–224, <https://doi.org/10.1002/jame.20026>, 2013.

628 Shangguan, W., Hengl, T., Mendes de Jesus, J., Yuan, H., and Dai, Y.: Mapping the global depth to
 629 bedrock for land surface modeling: GLOBAL MAP OF DEPTH TO BEDROCK, *J. Adv. Model.*

630 Earth Syst., 9, 65–88, <https://doi.org/10.1002/2016MS000686>, 2017.

631 Singh, A., Serbin, S. P., McNeil, B. E., Kingdon, C. C., and Townsend, P. A.: Imaging spectroscopy
632 algorithms for mapping canopy foliar chemical and morphological traits and their uncertainties,
633 Ecological Applications, 25, 2180–2197, <https://doi.org/10.1890/14-2098.1>, 2015.

634 Skidmore, A. K., Ferwerda, J. G., Mutanga, O., Van Wieren, S. E., Peel, M., Grant, R. C., Prins, H.
635 H. T., Balcik, F. B., and Venus, V.: Forage quality of savannas — simultaneously mapping foliar
636 protein and polyphenols for trees and grass using hyperspectral imagery, Remote Sensing of
637 Environment, 114, 64–72, <https://doi.org/10.1016/j.rse.2009.08.010>, 2010.

638 Sun, Y., Peng, S., Goll, D. S., Ciais, P., Guenet, B., Guimberteau, M., Hinsinger, P., Janssens, I. A.,
639 Peñuelas, J., Piao, S., Poulter, B., Violette, A., Yang, X., Yin, Y., and Zeng, H.: Diagnosing
640 phosphorus limitations in natural terrestrial ecosystems in carbon cycle models, 5, 730–749,
641 <https://doi.org/10.1002/2016EF000472>, 2017.

642 Tang, X., Zhao, X., Bai, Y., Tang, Z., Wang, W., Zhao, Y., Wan, H., Xie, Z., Shi, X., Wu, B., Wang,
643 G., Yan, J., Ma, K., Du, S., Li, S., Han, S., Ma, Y., Hu, H., He, N., Yang, Y., Han, W., He, H., Yu, G.,
644 Fang, J., and Zhou, G.: Carbon pools in China’s terrestrial ecosystems: New estimates based on an
645 intensive field survey, Proc Natl Acad Sci USA, 115, 4021–4026,
646 <https://doi.org/10.1073/pnas.1700291115>, 2018a.

647 Tang, Z., Xu, W., Zhou, G., Bai, Y., Li, J., Tang, X., Chen, D., Liu, Q., Ma, W., Xiong, G., He, H.,
648 He, N., Guo, Y., Guo, Q., Zhu, J., Han, W., Hu, H., Fang, J., and Xie, Z.: Patterns of plant carbon,
649 nitrogen, and phosphorus concentration in relation to productivity in China’s terrestrial ecosystems,
650 Proc. Natl. Acad. Sci. U. S. A., 115, 4033–4038, <https://doi.org/10.1073/pnas.1700295114>, 2018b.

651 Terrer, C., Jackson, R. B., Prentice, I. C., Keenan, T. F., Kaiser, C., Vicca, S., Fisher, J. B., Reich, P.
652 B., Stocker, B. D., Hungate, B. A., Peñuelas, J., McCallum, I., Soudzilovskaia, N. A., Cernusak, L.
653 A., Talhelm, A. F., Van Sundert, K., Piao, S., Newton, P. C. D., Hovenden, M. J., Blumenthal, D. M.,
654 Liu, Y. Y., Müller, C., Winter, K., Field, C. B., Viechtbauer, W., Van Lissa, C. J., Hoosbeek, M. R.,
655 Watanabe, M., Koike, T., Leshyk, V. O., Polley, H. W., and Franklin, O.: Nitrogen and phosphorus
656 constrain the CO₂ fertilization of global plant biomass, Nat. Clim. Chang., 9, 684–689,
657 <https://doi.org/10.1038/s41558-019-0545-2>, 2019.

658 Thornton, P. E., Lamarque, J.-F., Rosenbloom, N. A., and Mahowald, N. M.: Influence of carbon-
 659 nitrogen cycle coupling on land model response to CO₂ fertilization and climate variability, *Glob.*
 660 *Biogeochem. Cycle*, 21, <https://doi.org/10.1029/2006GB002868>, 2007.

661 Vincent, A. G., Sundqvist, M. K., Wardle, D. A., and Giesler, R.: Bioavailable soil phosphorus
 662 decreases with increasing elevation in a subarctic tundra landscape, *PLoS One*, 9, e92942,
 663 <https://doi.org/10.1371/journal.pone.0092942>, 2014.

664 Vitousek, P.: Nutrient Cycling and Nutrient Use Efficiency, *Am. Nat.*, 119, 553–572,
 665 <https://doi.org/10.1086/283931>, 1982.

666 Vitousek, P. M. and Howarth, R. W.: Nitrogen limitation on land and in the sea: How can it occur?,
 667 *Biogeochemistry*, 13, 87–115, <https://doi.org/10.1007/BF00002772>, 1991.

668 Vitousek, P. M., Porder, S., Houlton, B. Z., and Chadwick, O. A.: Terrestrial phosphorus limitation:
 669 mechanisms, implications, and nitrogen—phosphorus interactions, 20, 5–15, 2010.

670 Walker, T. W. and Syers, J. K.: The fate of phosphorus during pedogenesis, *Geoderma*, 15, 1–19,
 671 [https://doi.org/10.1016/0016-7061\(76\)90066-5](https://doi.org/10.1016/0016-7061(76)90066-5), 1976.

672 Wang, Z., Townsend, P. A., Schweiger, A. K., Couture, J. J., Singh, A., Hobbie, S. E., and Cavender-
 673 Bares, J.: Mapping foliar functional traits and their uncertainties across three years in a grassland
 674 experiment, *Remote Sensing of Environment*, 221, 405–416,
 675 <https://doi.org/10.1016/j.rse.2018.11.016>, 2019.

676 Wieder, W. R., Cleveland, C. C., Smith, W. K., and Todd-Brown, K.: Future productivity and carbon
 677 storage limited by terrestrial nutrient availability, *Nat. Geosci.*, 8, 441–444,
 678 <https://doi.org/10.1038/ngeo2413>, 2015.

679 Xu, L., He, N., and Yu, G.: Nitrogen storage in China’s terrestrial ecosystems, *Science of The Total*
 680 *Environment*, 709, 136201, <https://doi.org/10.1016/j.scitotenv.2019.136201>, 2020.

681 Yang, Y.-H., Ma, W.-H., Mohammat, A., and Fang, J.-Y.: Storage, Patterns and Controls of Soil
 682 Nitrogen in China, *Pedosphere*, 17, 776–785, [https://doi.org/10.1016/S1002-0160\(07\)60093-9](https://doi.org/10.1016/S1002-0160(07)60093-9),
 683 2007.

684 Zhang, C., Tian, H., Liu, J., Wang, S., Liu, M., Pan, S., and Shi, X.: Pools and distributions of soil
685 phosphorus in China, *Glob. Biogeochem. Cycle*, 19, GB1020,
686 <https://doi.org/10.1029/2004GB002296>, 2005.

687 Zhang, J., Zhao, N., Liu, C., Yang, H., Li, M., Yu, G., Wilcox, K., Yu, Q., and He, N.: C:N:P
688 stoichiometry in China's forests: From organs to ecosystems, *Funct. Ecol.*, 32, 50–60,
689 <https://doi.org/10.1111/1365-2435.12979>, 2018.

690 Zhang, Y.-W., Guo, Y., Tang, Z., Feng, Y., Zhu, X., Xu, W., Bai, Y., Zhou, G., Xie, Z., Fang, J.: Patterns
691 of nitrogen and phosphorus pools in terrestrial ecosystems in China, *Dryad, Dataset*,
692 <https://datadryad.org/stash/share/78EBjhBqNoam2jOSoO1AXvbZtgIpCTi9eT-eGE7wyOk>, 2020.

693

Table.1. N and P stocks of vegetation, litter, soil and total ecosystem in forest, shrublands and grasslands in China.

Vegetation type group	Vegetation type	Area (10 ⁶ ha)	N pool (10 ⁶ Mg N)				P pool (10 ⁶ Mg P)			
			Vegetation	Soil	Litter	Ecosystem	Vegetation	Soil	Litter	Ecosystem
Forest	EBF	45.5940. <u>6</u>	13.0818. <u>0</u>	587.48476.4	1.937	608.73496 <u>1</u>	1.897	193.27154. <u>8</u>	0.101	195.26156 <u>6</u>
	DBF	91.1466. <u>3</u>	43.431	665.60811.3	4.253.	713.29858 <u>1</u>	8.376.9	277.61346 <u>5</u>	0.744	286.71353 <u>8</u>
	ENF	99.9783. <u>8</u>	34.9328. <u>4</u>	1074.18952. <u>8</u>	3.582.	1112.6998 <u>4</u>	5.593.7	377.27349 <u>2</u>	0.232	383.08353 <u>1</u>
	DNF	19.7911. <u>5</u>	7.535.6	84.76177.7	1.730.	94.03183. <u>8</u>	4.611.5	123.3373. <u>6</u>	0.751	128.7075. <u>2</u>
	MF	13.259.6	4.647	96.95107.6	0.655	104.07112 <u>8</u>	1.380.9	42.0841.5	0.131	43.5942.4
	<i>subtotal</i>	269.752 <u>11.9</u>	111.699 <u>9.8</u>	2508.98252 <u>5.8</u>	12.14 <u>9.3</u>	2632.8026 <u>34.9</u>	21.8414.6	1013.5596 <u>5.6</u>	1.960.9	1037.3498 <u>1.1</u>
Shrubland	EBS	21.6518. <u>7</u>	2.156	160.54213 <u>6</u>	0.645	162.70216 <u>2</u>	0.202	52.9580.9	<0.031	53.1881.1
	DBS	63.9448. <u>7</u>	5.305	598.39570 <u>9</u>	1.402	605.09577 <u>6</u>	0.585	220.48233 <u>6</u>	0.091	221.15234 <u>2</u>
	ENS	1.360	0.061	13.2912.4	<0.041	13.3612.5	<0.0081	5.404.9	≤	5.414.9
	SS	17.3511. <u>9</u>	0.225	48.66.1	0.211	49.1066.7	<0.021	81.8561.6	0.00061	81.8861.6
	<i>subtotal</i>	104.348 <u>0.3</u>	7.148.1	820.88863 <u>0</u>	2.237.8	830.24873 <u>0</u>	0.807	360.69381 <u>0</u>	0.131	361.62381 <u>8</u>

Grassland	ME	<u>59.6244.</u> <u>2</u>	<u>47.8711.</u> <u>6</u>	<u>994.79806</u> <u>.9</u>	<u>0.431</u>	<u>4012.7981</u> <u>8.5</u>	<u>4.330.9</u> <u>2</u>	<u>217.20247</u> <u>2</u>	<u>≤</u> <u>0.0051</u>	<u>218.54248</u> <u>.0</u>
	ST	<u>490.081</u> <u>37.4</u>	<u>36.3421.</u> <u>3</u>	<u>4562.9413</u> <u>48.5</u>	<u>0.223</u>	<u>4599.4713</u> <u>70.1</u>	<u>2.321.5</u> <u>0.262</u>	<u>569.27573</u> <u>84.44112.</u>	<u><0.021</u> <u>≤0.041</u>	<u>574.64574</u> <u>84.74113.</u>
	TU	<u>24.3922.</u> <u>8</u>	<u>2.393</u> <u>2</u>	<u>471.02230</u> <u>.4</u>	<u>0.401</u>	<u>473.51232</u> <u>.8</u>	<u>0.262</u> <u>9</u>	<u>84.44112.</u> <u>9</u>	<u><0.041</u> <u>2</u>	<u>84.74113.</u> <u>2</u>
	SG	<u>439.271</u> <u>03.8</u>	<u>40.7813.</u> <u>6</u>	<u>4376.0286</u> <u>0.6</u>	<u>0.091</u>	<u>4416.8987</u> <u>4.4</u>	<u>2.330.9</u> <u>6.3</u>	<u>4576.4850</u> <u>6.3</u>	<u><0.021</u> <u>7.2</u>	<u>4578.8350</u> <u>7.2</u>
	<i>subtotal</i>	<u>413.353</u> <u>08.2</u>	<u>97.3548.</u> <u>8</u>	<u>4104.6832</u> <u>46.4</u>	<u>0.556</u>	<u>4202.5832</u> <u>95.8</u>	<u>6.243.5</u> <u>39.5</u>	<u>2447.4414</u> <u>39.5</u>	<u><0.051</u> <u>43.0</u>	<u>2453.7014</u> <u>43.0</u>
Total		<u>787600.</u> <u>4</u>	<u>216.171</u> <u>56.7</u>	<u>7434.5366</u> <u>35.2</u>	<u>44.9211.</u> <u>7</u>	<u>7665.6267</u> <u>93.1</u>	<u>28.8818.8</u> <u>86.1</u>	<u>3821.6427</u> <u>86.1</u>	<u>2.141.0</u> <u>06.0</u>	<u>3852.6628</u> <u>06.0</u>

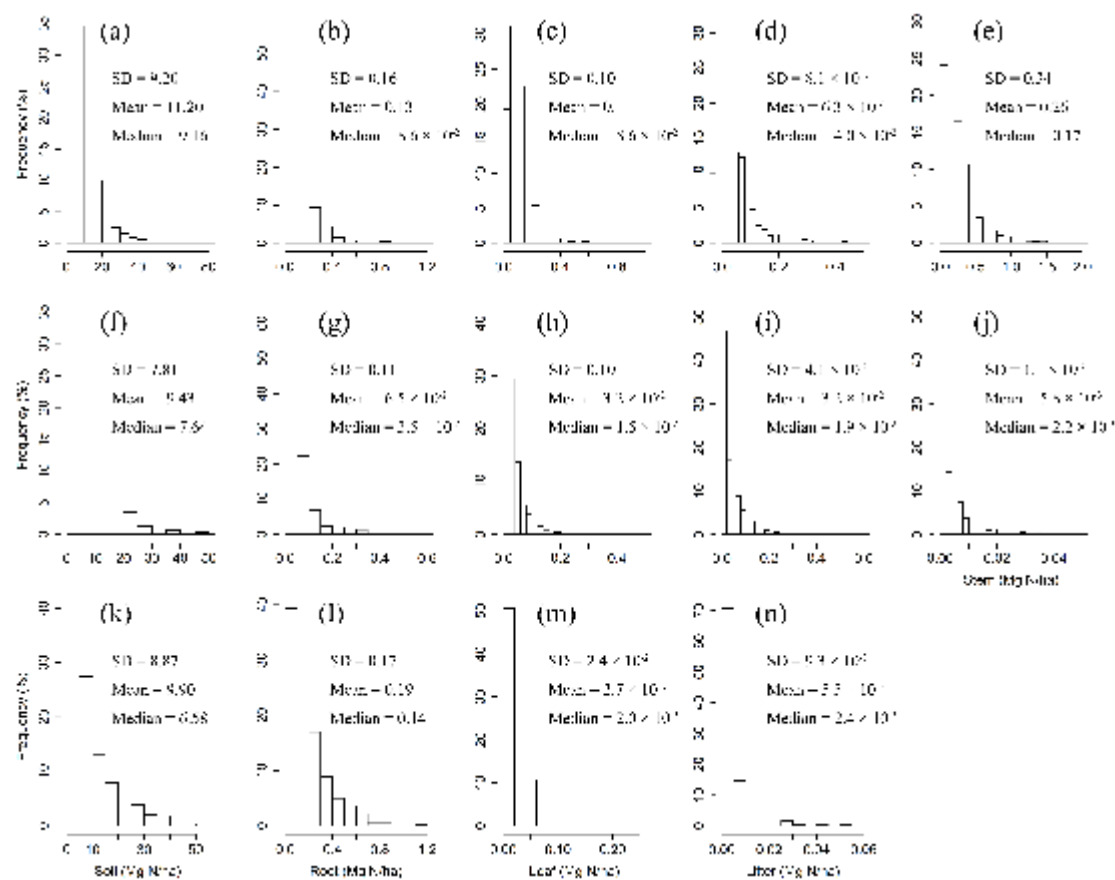
695 EBF, evergreen broadleaf forest; DBF, deciduous broadleaf forest; ENF, evergreen needle-leaf forest; DNF, deciduous needle-

696 leaf forest; MF, broadleaf and needle-leaf forest; EBS, evergreen broadleaf shrub; DBS, deciduous broadleaf shrub; ENS,

697 evergreen needle-leaf shrub; SS, sparse shrub; ME, meadow; ST, steppe; TU, tussock; and SG, sparse grassland.

Table.2. N and P stocks of plant organs (leaf, stem and root) in forest forests, shrublands and grasslands in China.								
Vegetation type group	Vegetation type	Area (10 ⁶ ha)	N pool (40 ⁶ Mg Tg)			P pool (40 ⁶ Mg Tg)		
			Leaf	Stem	Root	Leaf	Stem	Root
Forest	EBF	45.5940.6	3.8499	10.8631	4.6140	0.2733	1.3080	0.3133
	DBF	91.1466.3	6.8201	23.28926.6	13.32210.5	0.5556	4.6806	3.1331.6
	ENF	99.9783.8	10.1858.6	17.09013.4	7.6536.4	1.2560.9	3.2052.0	1.1250.8
	DNF	19.7911.5	1.6613	4.3362.9	1.5354	0.2922	3.6910.9	0.6313
	MF	13.259.6	1.3260	3.7142.6	1.4280	0.1171	0.9317	0.3282
	subtotal	269.75211.9	23.84421.0	59.29355.5	28.55233.4	2.4931	13.8149.2	5.5313.3
Shrubland	EBS	21.6518.7	0.6326	0.0517	0.8727	≤0.0451	0.0741	0.0831
	DBS	63.9448.7	1.6824	0.2051.4	3.4132.7	0.1241	0.1641	0.2902
	ENS	1.360	≤0.0371	≤0.0011	≤0.0221	≤0.0051	≤0.00011	≤0.0031
	SS	17.3511.9	0.0701	0.0211	0.1293	≤0.0051	≤0.0051	≤0.0061
	subtotal	104.3180.3	2.4201	0.2792.3	4.4363.8	0.1792	0.2432	0.3822
eGrassland	ME	59.6244.2	1.1810.9	0.0	16.68710.7	0.1211	0.0	1.2130.8
	ST	190.08137.4	2.8182	0.0	33.49219.2	0.2612	0.0	2.0551.3
	TU	24.3922.8	0.5595	0.0	1.8307	0.0581	0.0	0.2012
	SG	139.27103.8	1.5731	0.0	39.21112.5	0.2441	0.0	2.0840.8
	subtotal	413.35308.2	6.1324.7	0.0	91.22044.1	0.6854	0.0	5.5533.1
Total		787600.4	32.39427.7	59.57157.8	124.20971.2	3.3572.7	14.0579.4	11.4666.7

See table 1 for abbreviations.



700

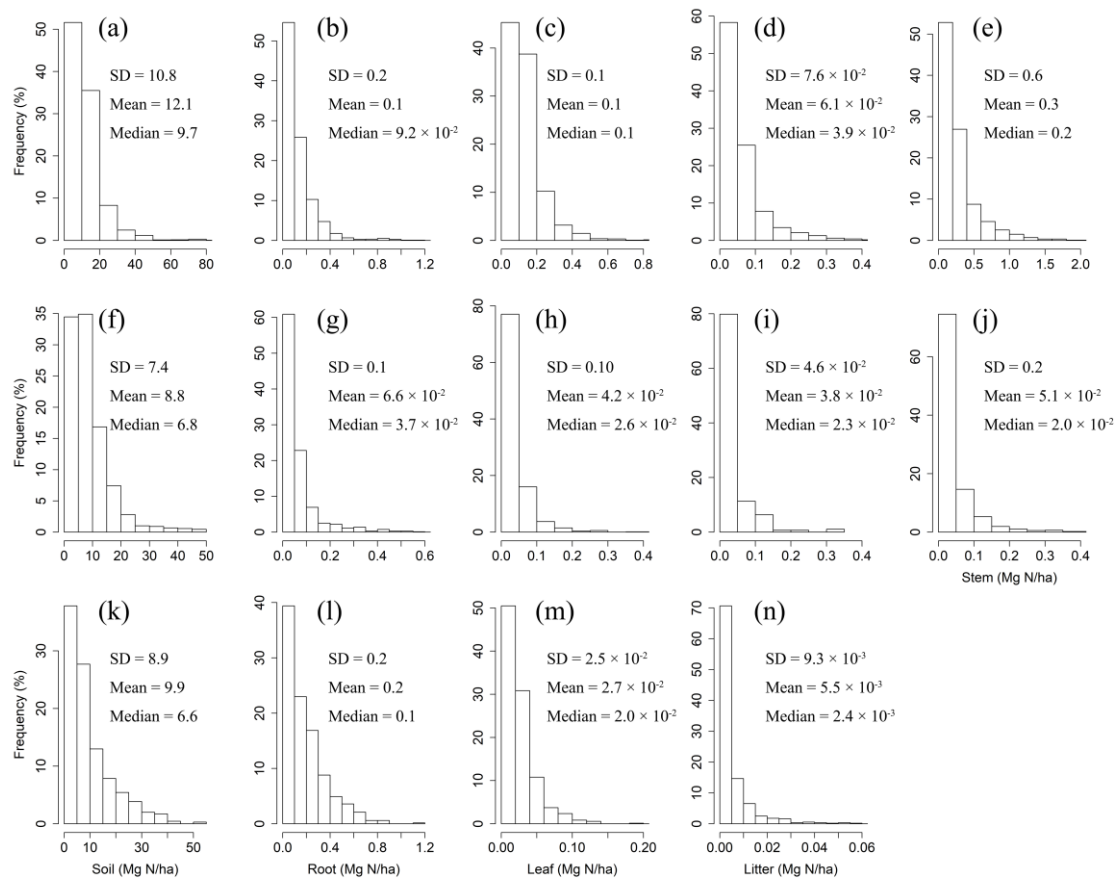
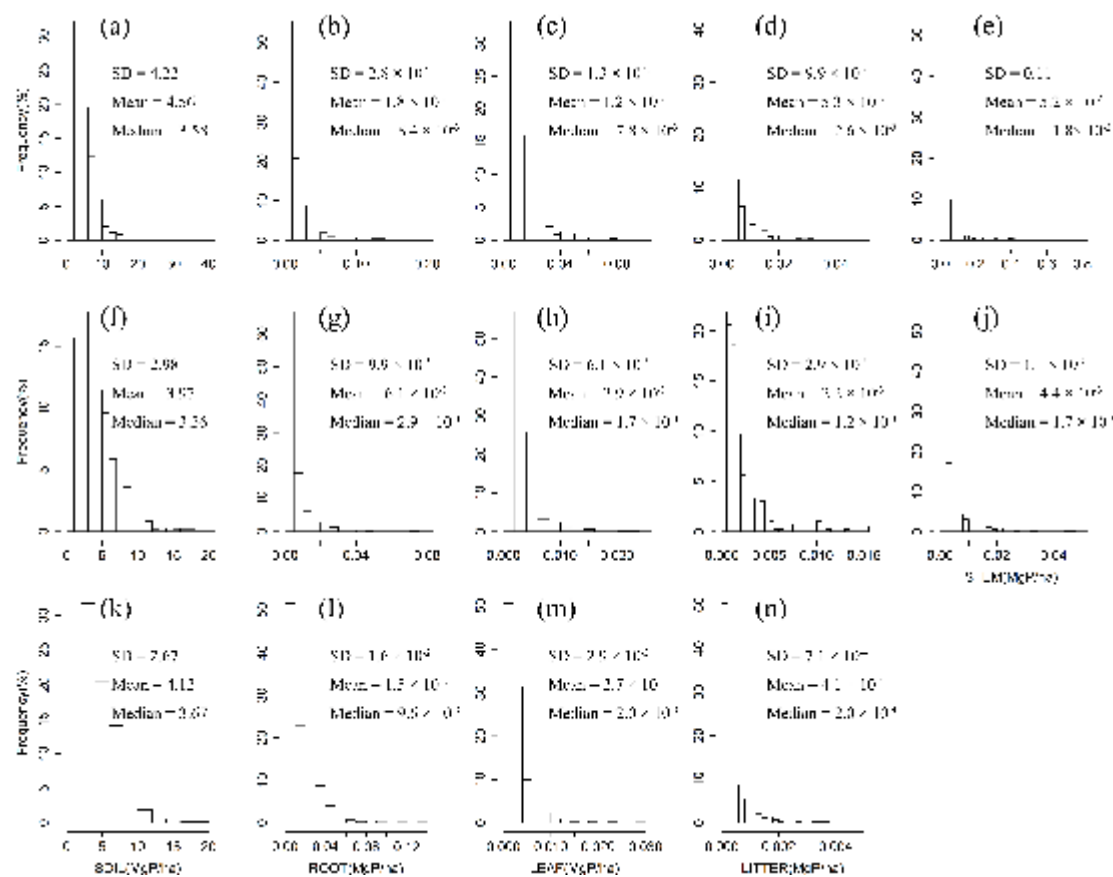


Fig. 1. Frequency distributions of N densities in soil, roots, leaves, litter and woody stems in forests (a–e), shrublands (f–j) and grasslands (k–n) in China.



704

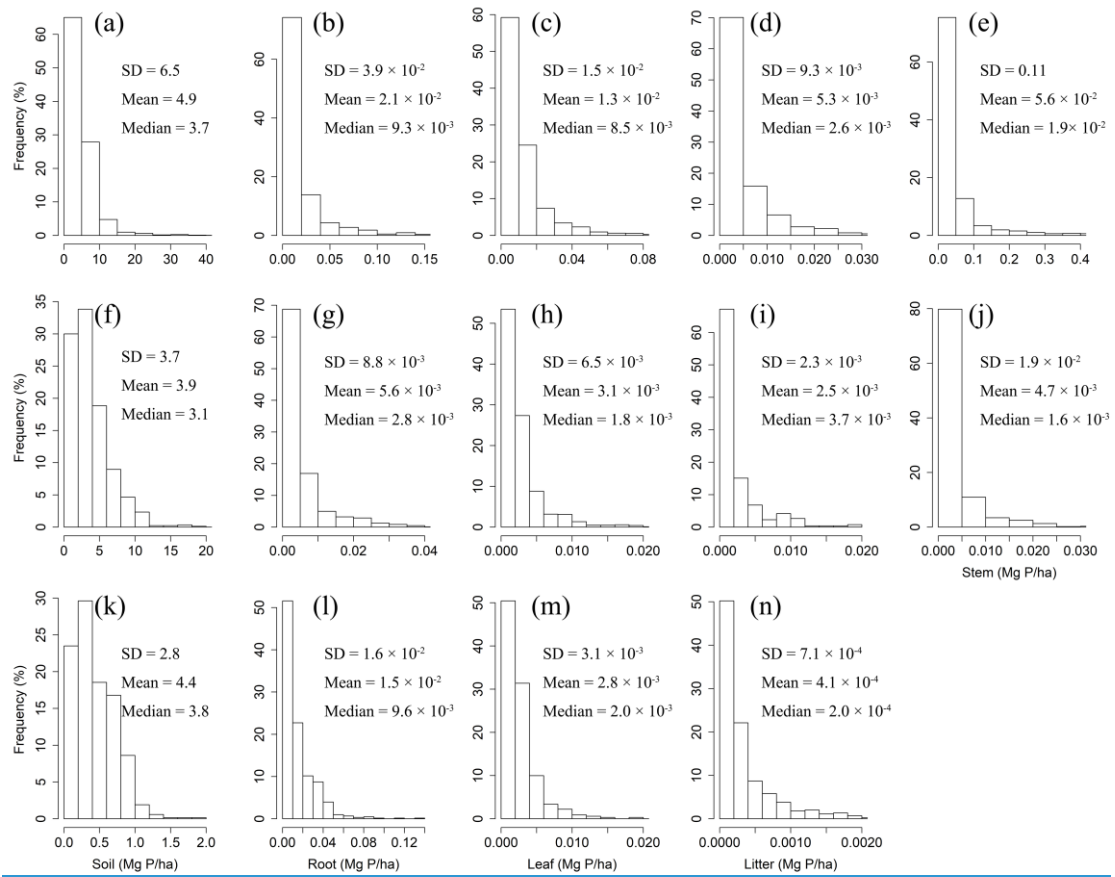
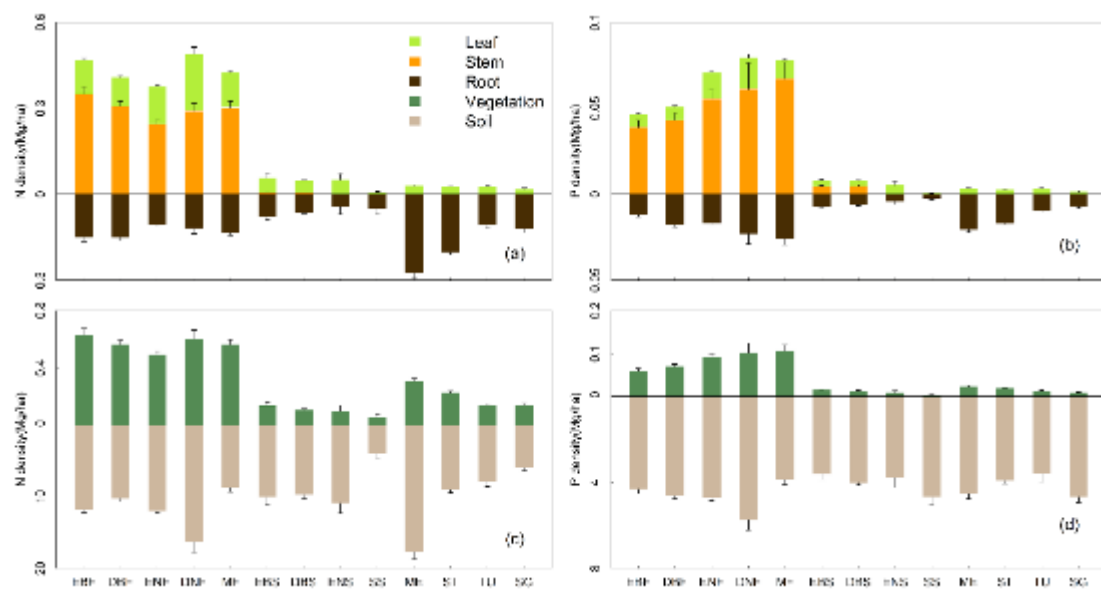


Fig. 2. Frequency distributions of P densities in soil, roots, leaves, litter and woody stems in forests (a–e), shrublands (f–j) and grasslands (k–n) in China.



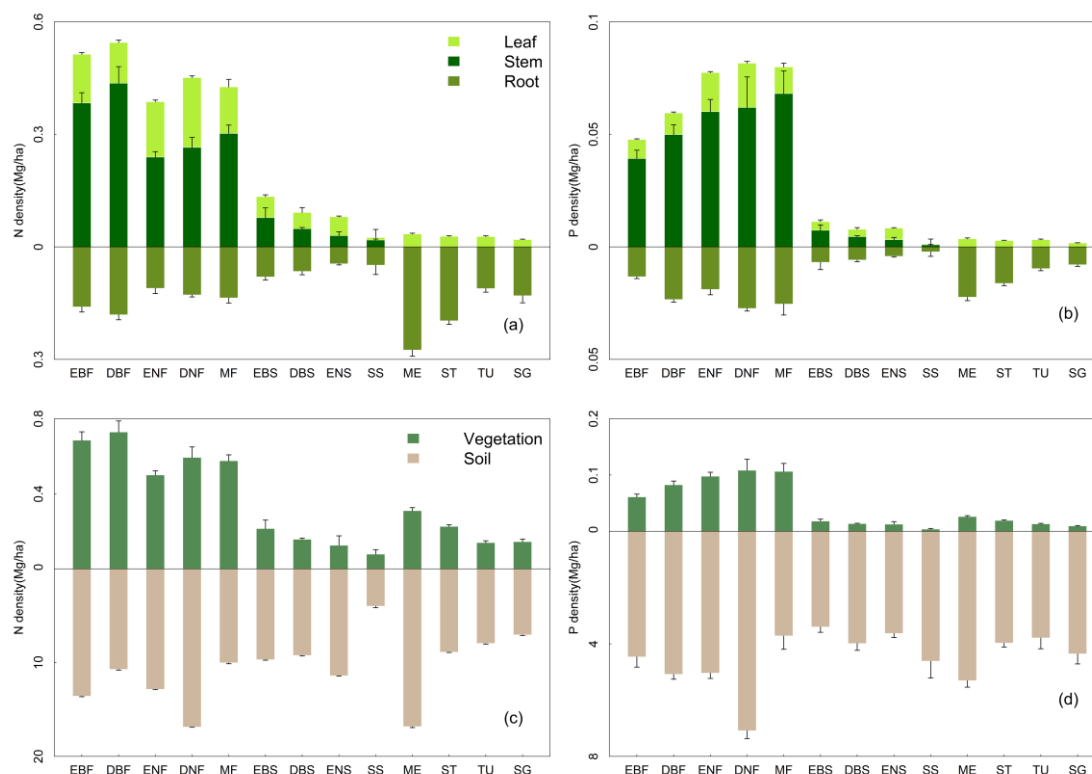
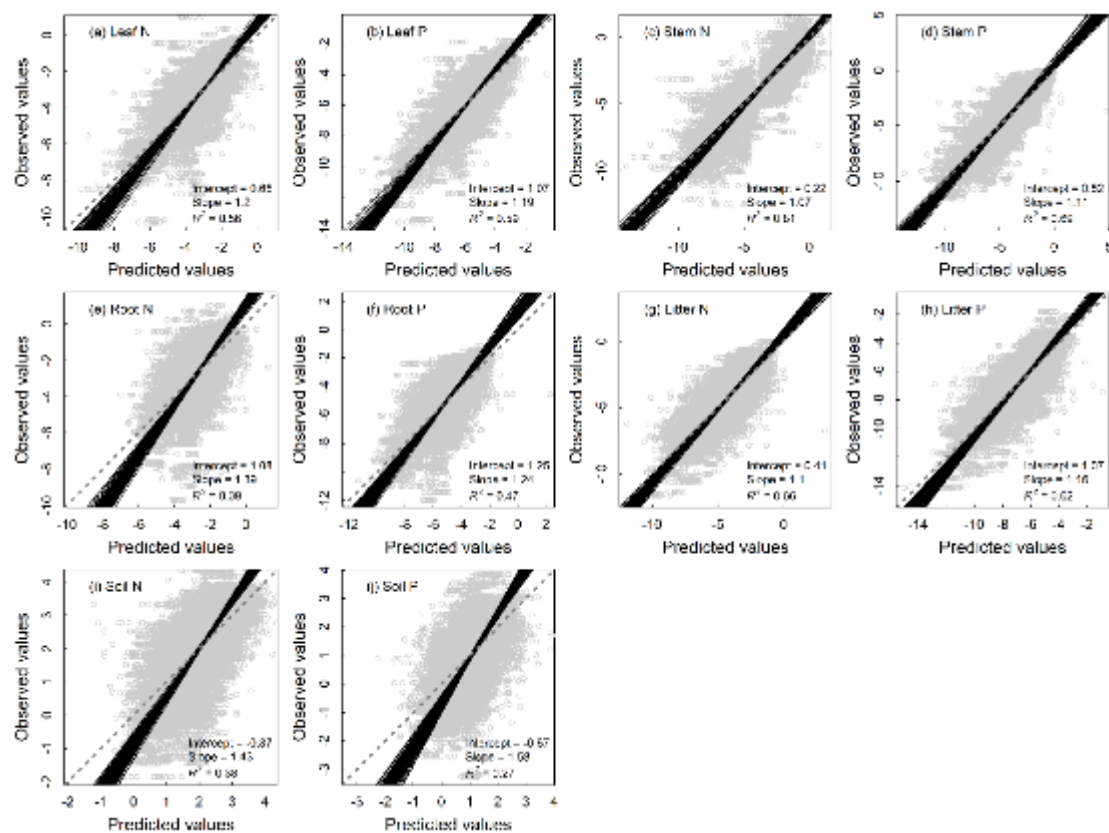


Fig. 3. N and P density allocations among leaf, stem and root (a & b) and between vegetation and soil (c & d) in 13 Vegetation types. See table 1 for abbreviations. The error bar represents standard error. Notice that the y axes above and below zero are disproportionate.



715

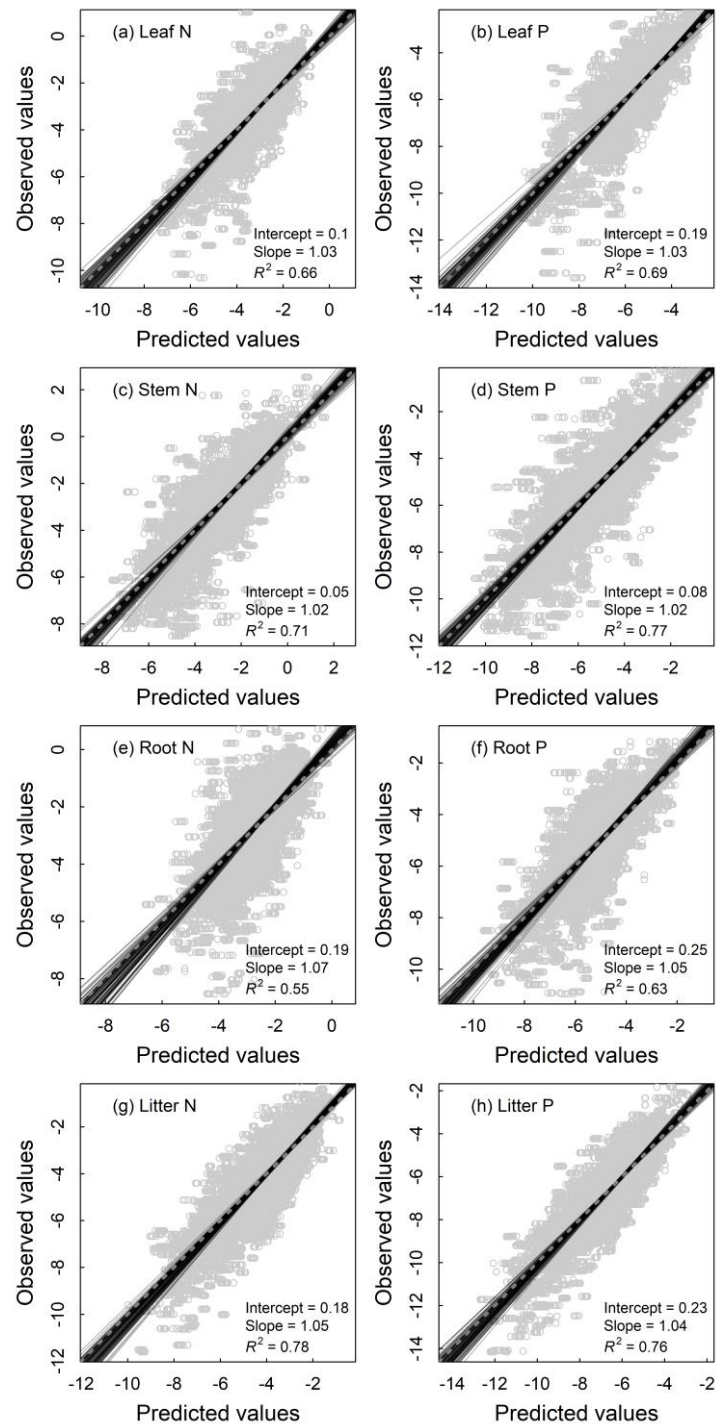
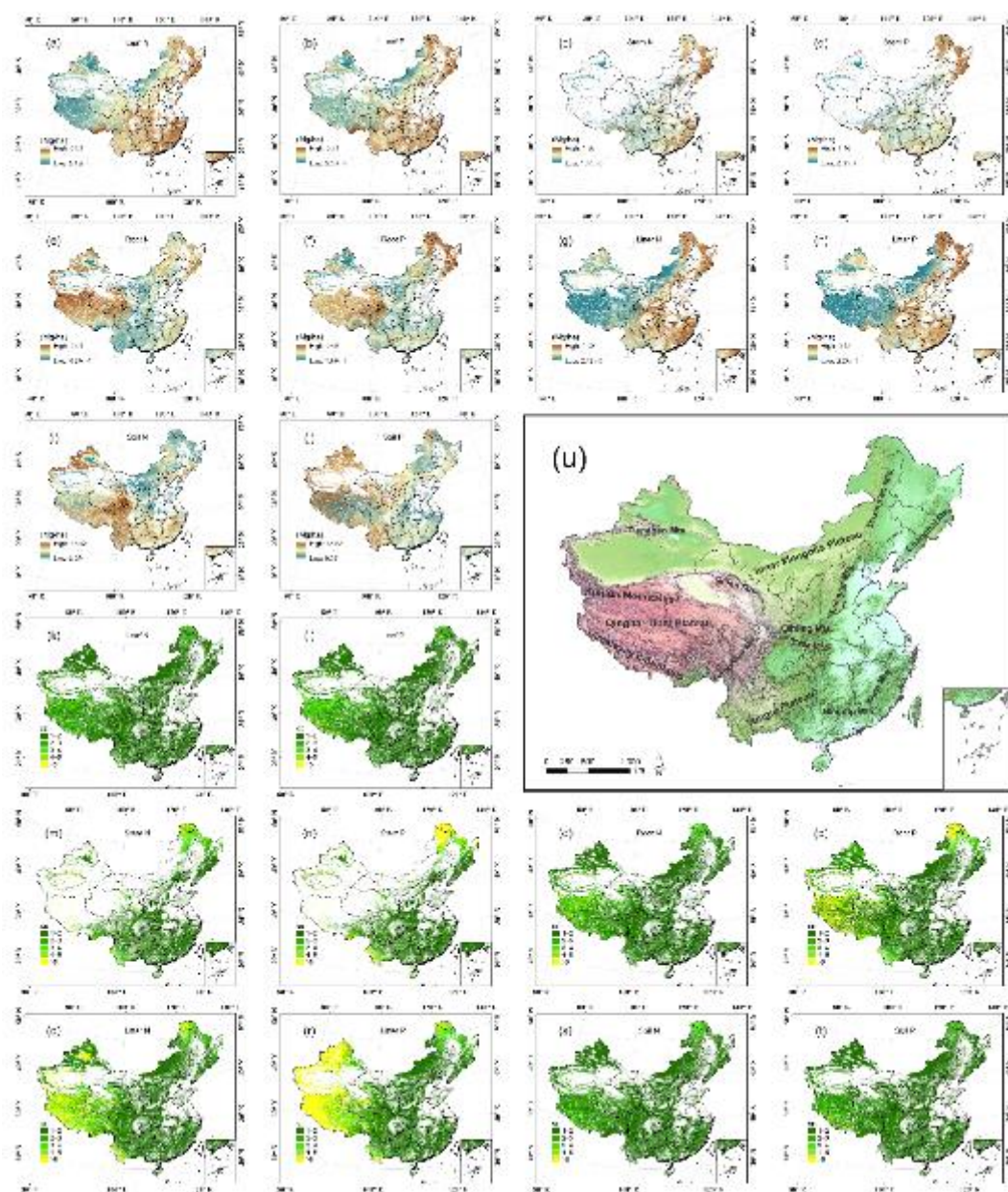


Fig. 4. Fitting performance of ~~artificial neural network~~random forest models for ~~different~~
~~components~~nutrient densities of leaves (a & b), woody stems (c & d), roots (e & f) and litter (g
& h) of terrestrial ecosystems in China based on 100 times of replications with the 10%
validation data. Solid lines represent all the fitting lines ~~by standard major axis regression~~, and
the displayed parameters stand for the average conditions. The dashed line denotes the 1:1 line.



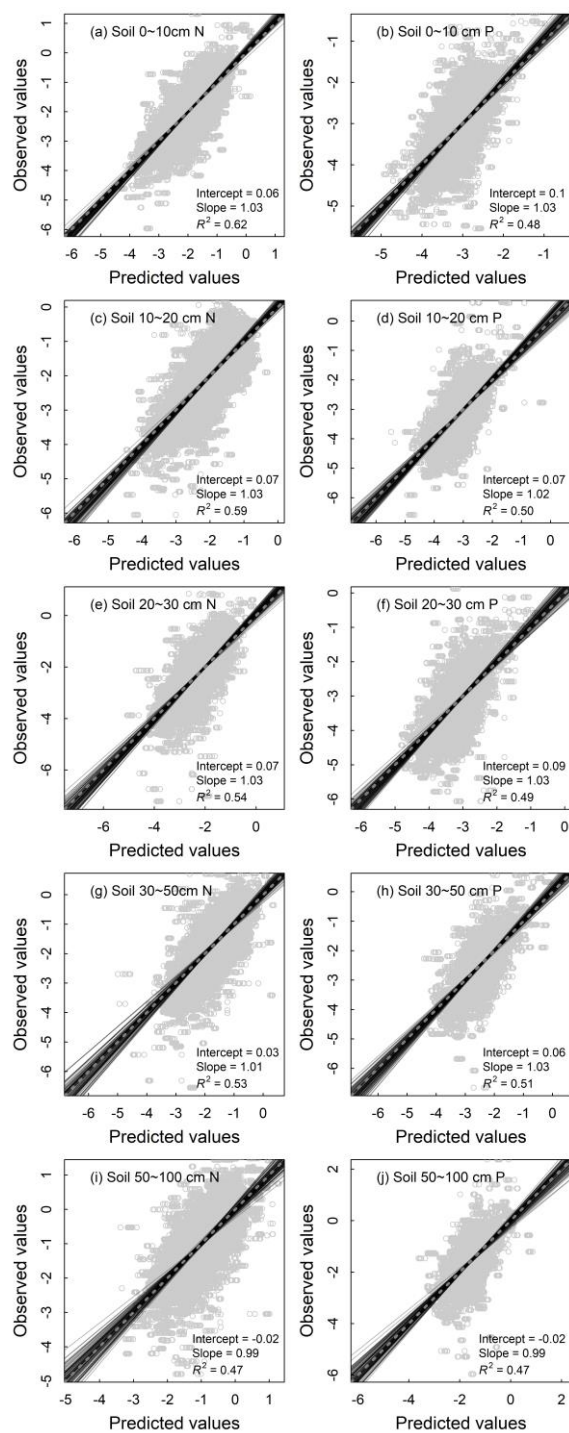


Fig. 5.

Fig. 5. Fitting performance of random forest models for nutrient densities of 0–10 cm (a & b), 10–20 cm (c & d), 20–30 cm (e & f), 30–50 cm (g & h) and 50–100 cm (i & j) soil layers of terrestrial ecosystems in China based on 100 times of replications with the 10% validation data. Solid lines represent all the fitting lines, and the displayed parameters stand for the average conditions. The dashed line denotes the 1:1 line.

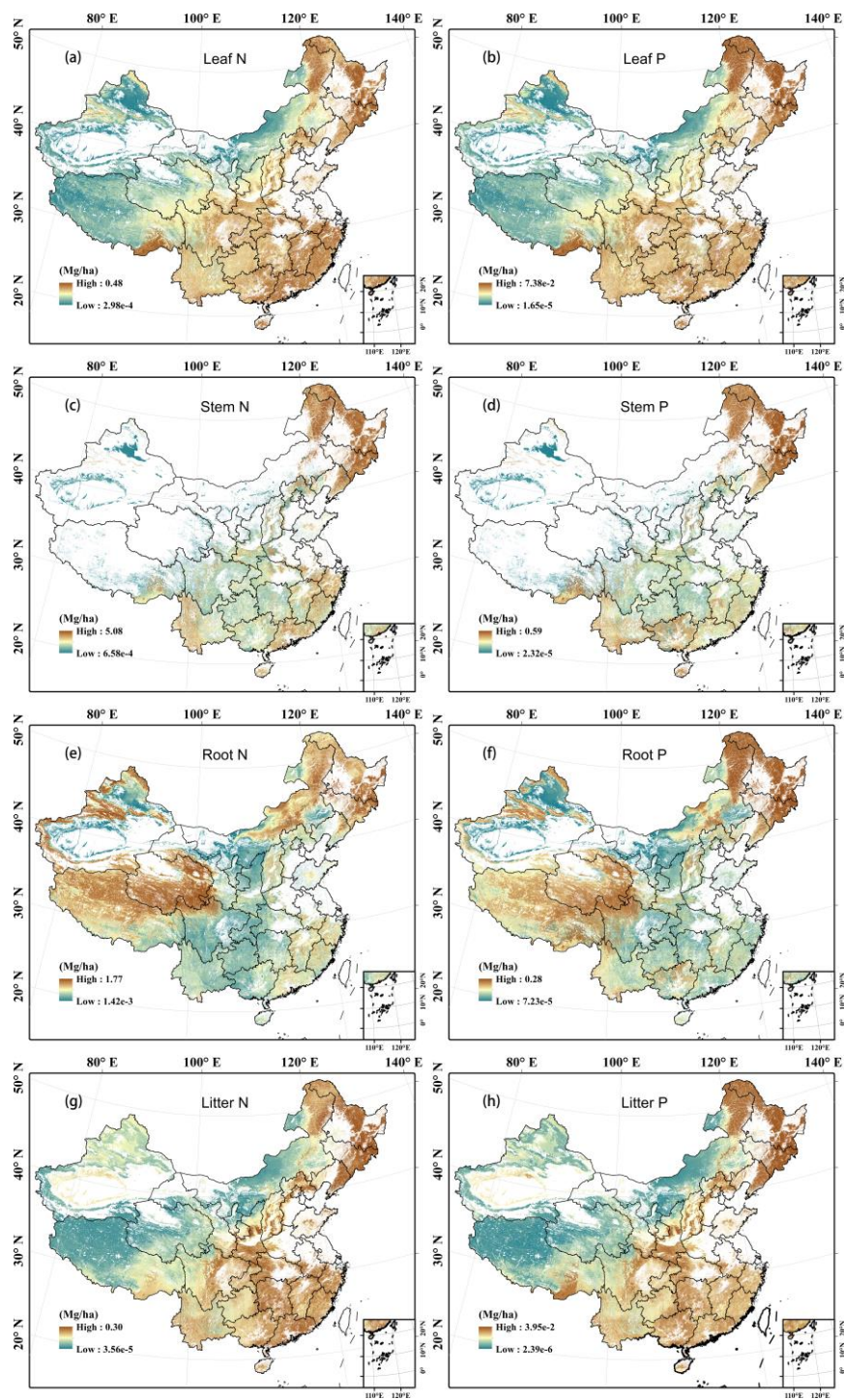
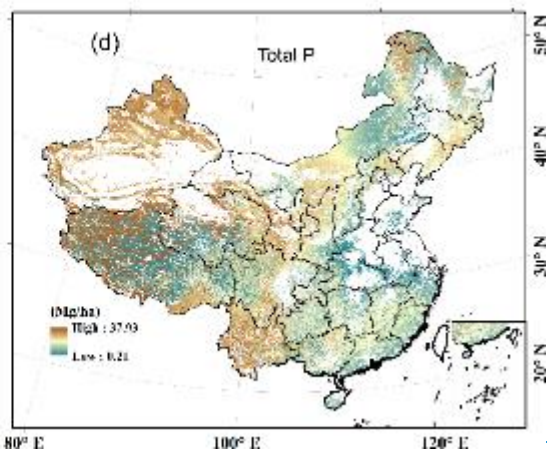
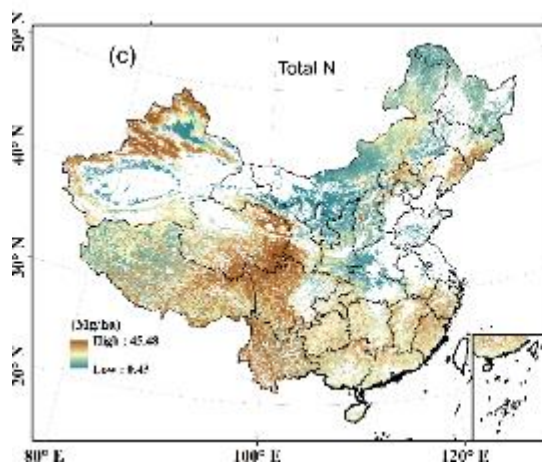
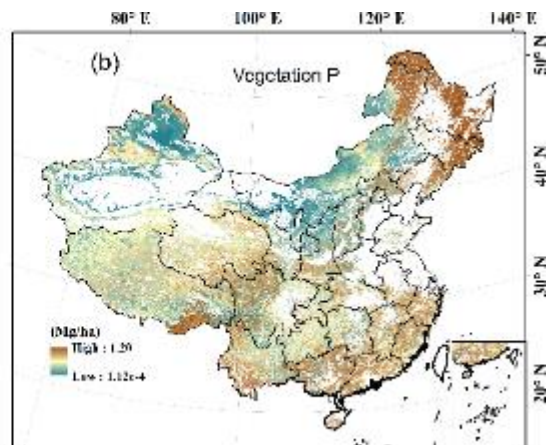
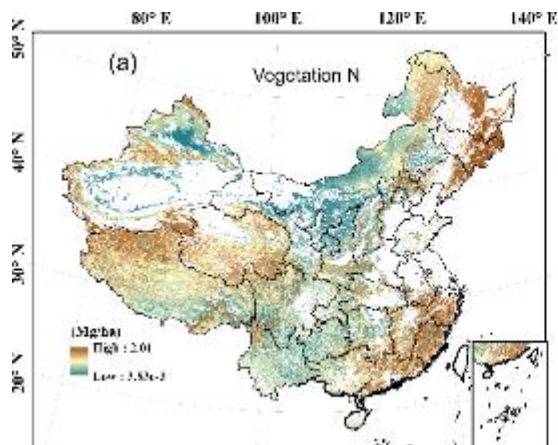


Fig. 6. Predicted spatial patterns of N and P densities with a resolution of 1 km (a–j) in leaves
(a & b), woody stems (c & d), roots (e & f) and their prediction standard deviations (SDs) (k–
t) in each component litter (g & h) of terrestrial ecosystems in China based on 100 replications.
The topographic map of China (u) is also shown.



737

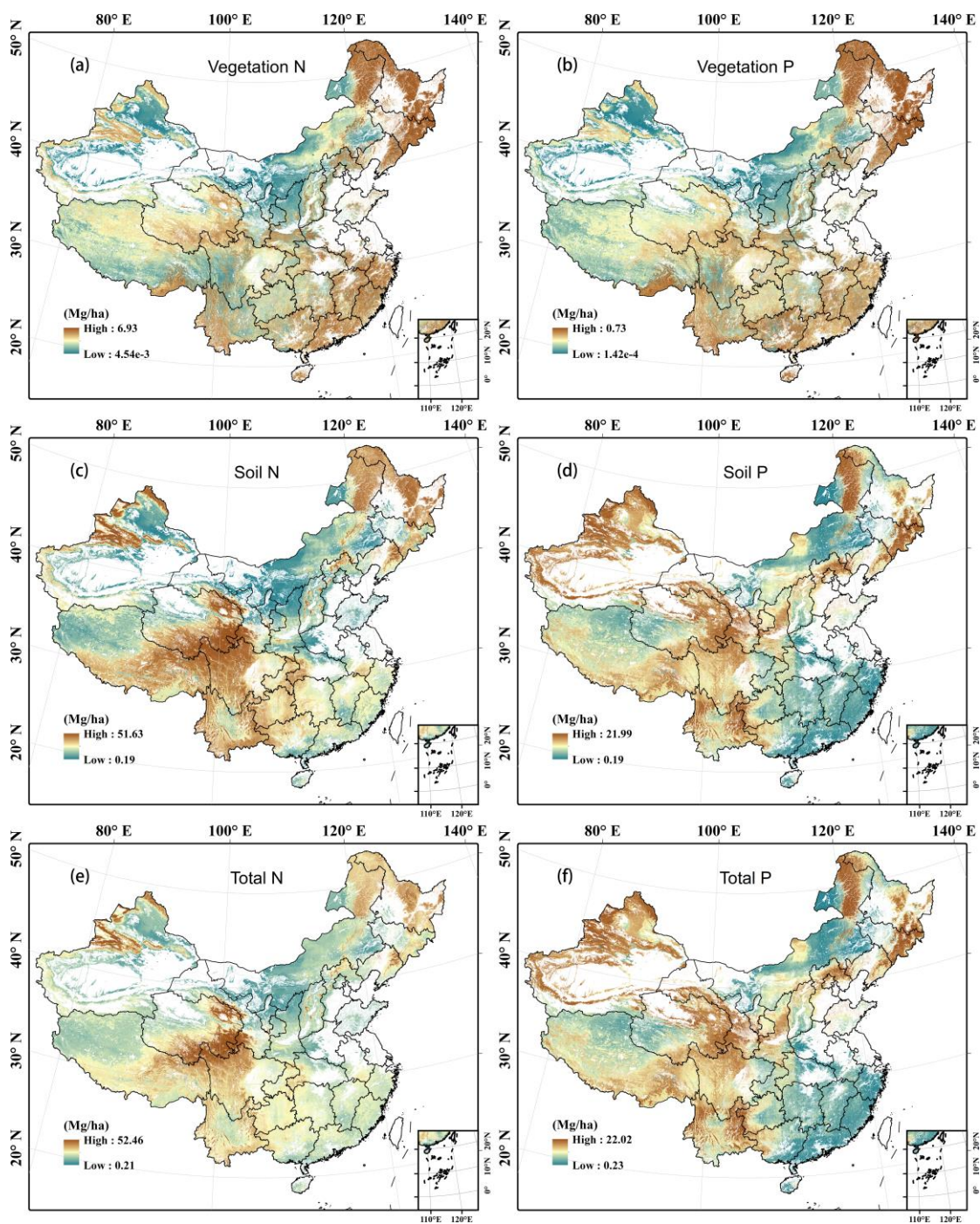


Fig. 6-~~Spatial~~7. Predicted spatial patterns of N and P densities with a resolution of 1 km in vegetation (a & b, the sum of leaves, stems and roots), soil (c & d, the sum of five layers) and ecosystems (~~e and de~~ e & f, the sum of ~~leaves, stems, roots~~ vegetation, litter and soil) of terrestrial ecosystems in China.

Supplement

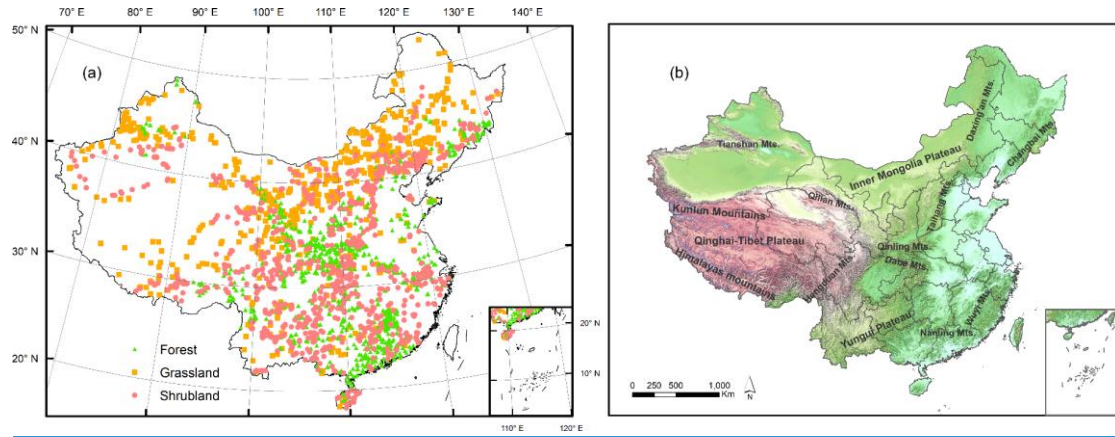


Fig. S1. The spatial distributions of sampling sites (a) and the topographic map of China (b).

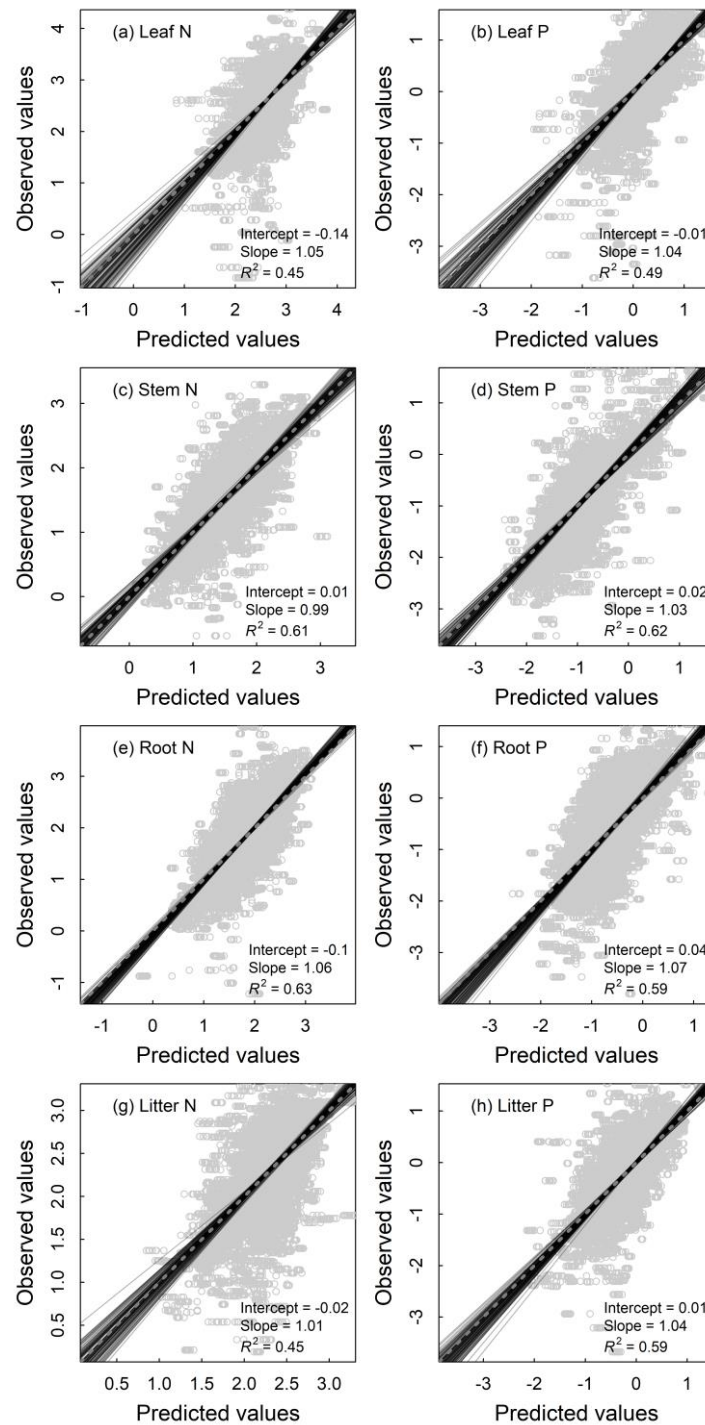


Fig. S2. Fitting performance of random forest models for nutrient concentrations of leaves (a & b), woody stems (c & d), roots (e & f) and litter (g & h) of terrestrial ecosystems in China based on 100 times of replications with the 10% validation data. Solid lines represent all the fitting lines, and the displayed parameters stand for the average conditions. The dashed line denotes the 1:1 line.

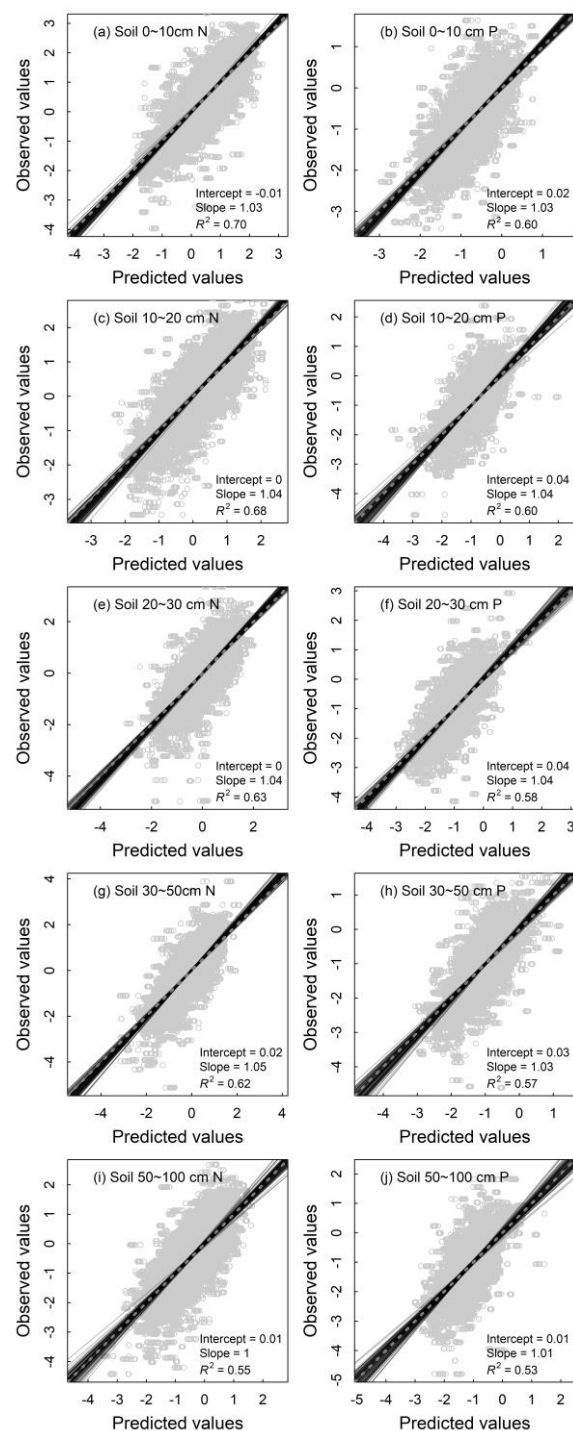


Fig. S3. Fitting performance of random forest models for nutrient concentrations of 0–10 cm (a & b), 10–20 cm (c & d), 20–30 cm (e & f), 30–50 cm (g & h) and 50–100 cm (i & j) soil layers of terrestrial ecosystems in China based on 100 times of replications with the 10% validation data. Solid lines represent all the fitting lines, and the displayed parameters stand for the average conditions. The dashed line denotes the 1:1 line.

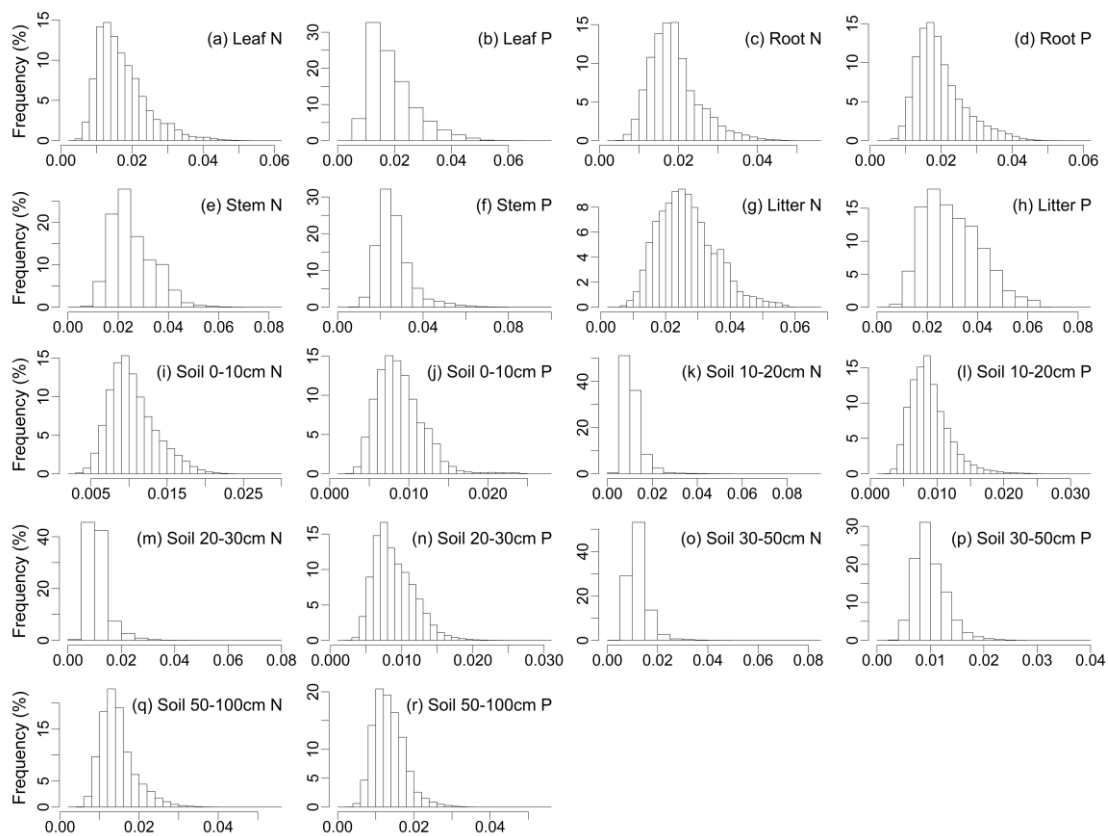


Fig. S4. Frequency distributions of standard deviations of the predictions in models for N and P densities in different components.

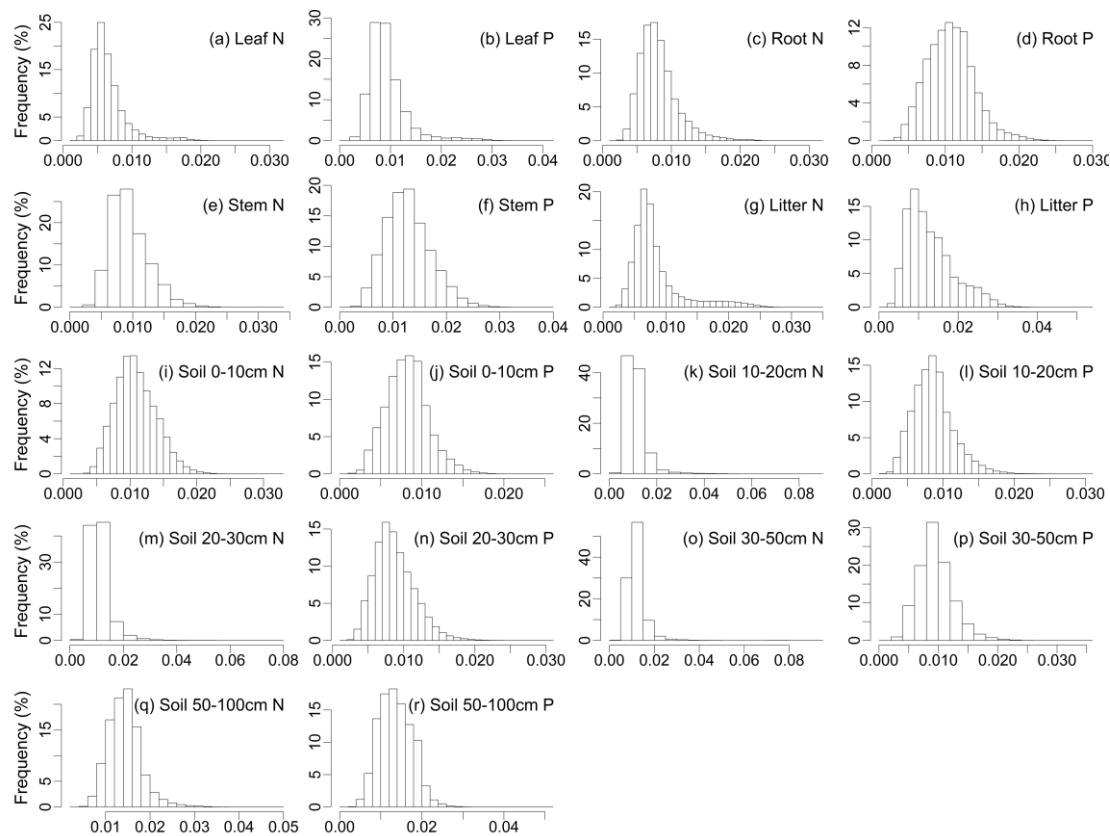


Fig. S5. Frequency distributions of standard deviations of the predictions in models for N and P concentrations in different components.

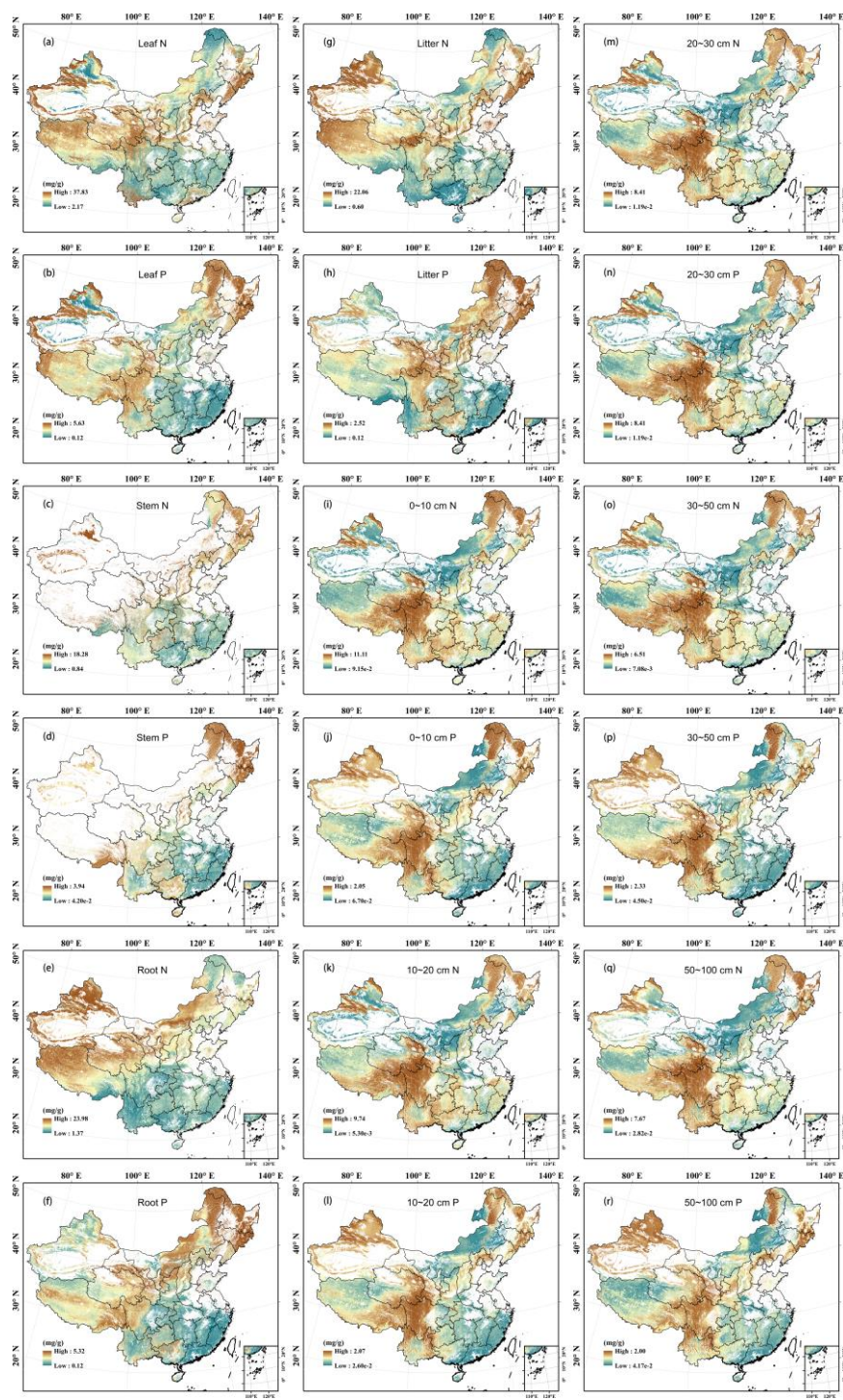


Fig. S6. Predicted spatial patterns of N and P concentrations with a resolution of 1 km (a–j) in
plant organs (a–f), litter (g & h), and soil layers (i–r) of terrestrial ecosystems in China.

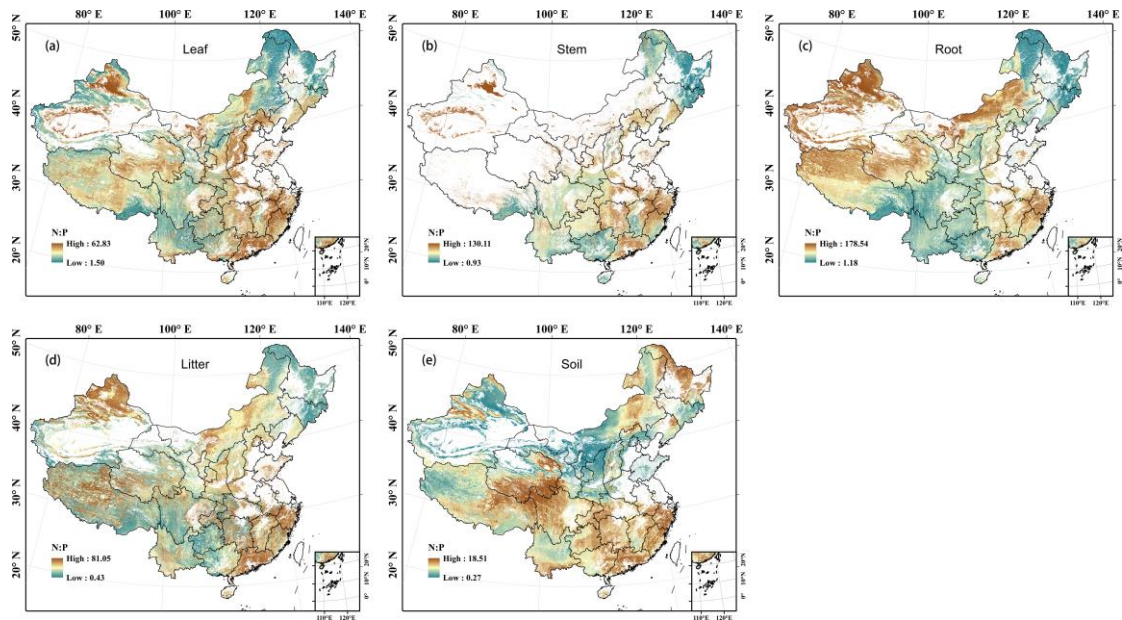


Fig. S7. Predicted spatial patterns of N:P ratios with a resolution of 1 km (a–j) in leaves (a), woody stems (b), roots (c), litter (d) and soil (e) of terrestrial ecosystems in China.

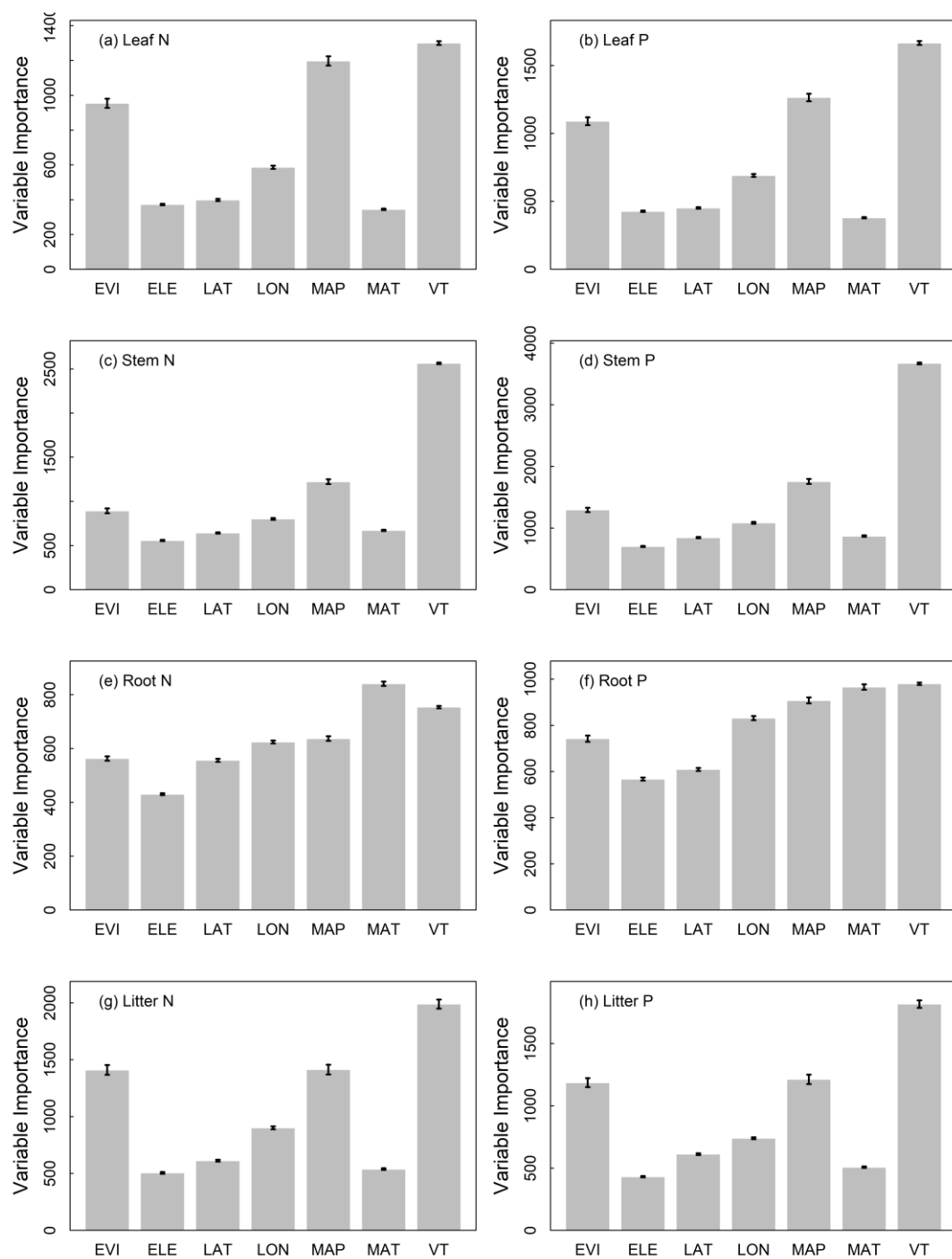


Fig. S8. The relative importance of variables in random forest models of N and P densities for
leaf (a & b), stem (c & d), root (e & f) and litter (g & h).

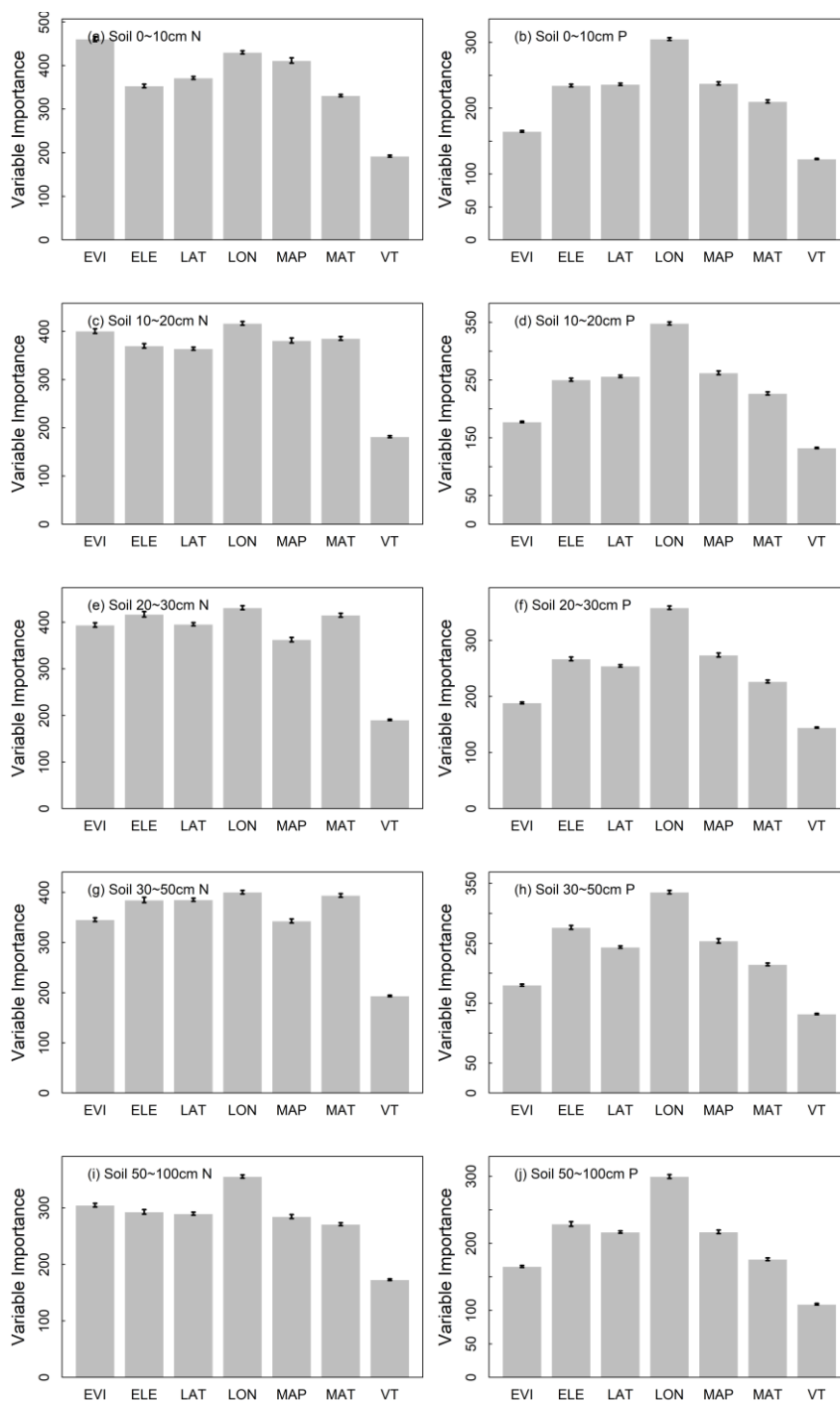


Fig. S9. The relative importance of variables in random forest models of N and P densities for 0-10 cm (a & b), 10-20 cm (c & d), 20-30 cm (e & f) 30-50 cm (g & h) and 50-100 cm (i & j) soil layers.

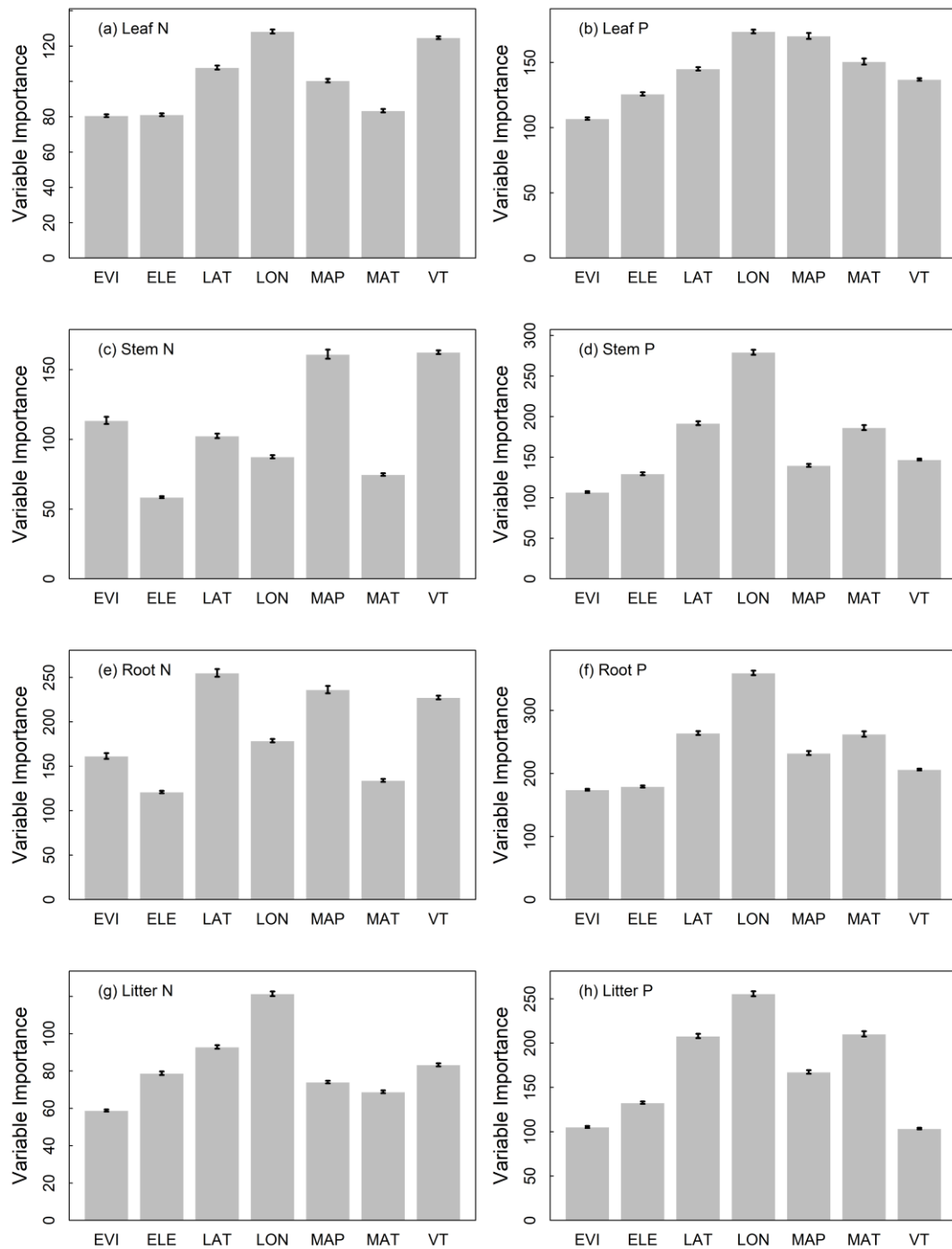


Fig. S10. The relative importance of variables in random forest models of N and P concentrations for leaf (a & b), stem (c & d), root (e & f) and litter (g & h).

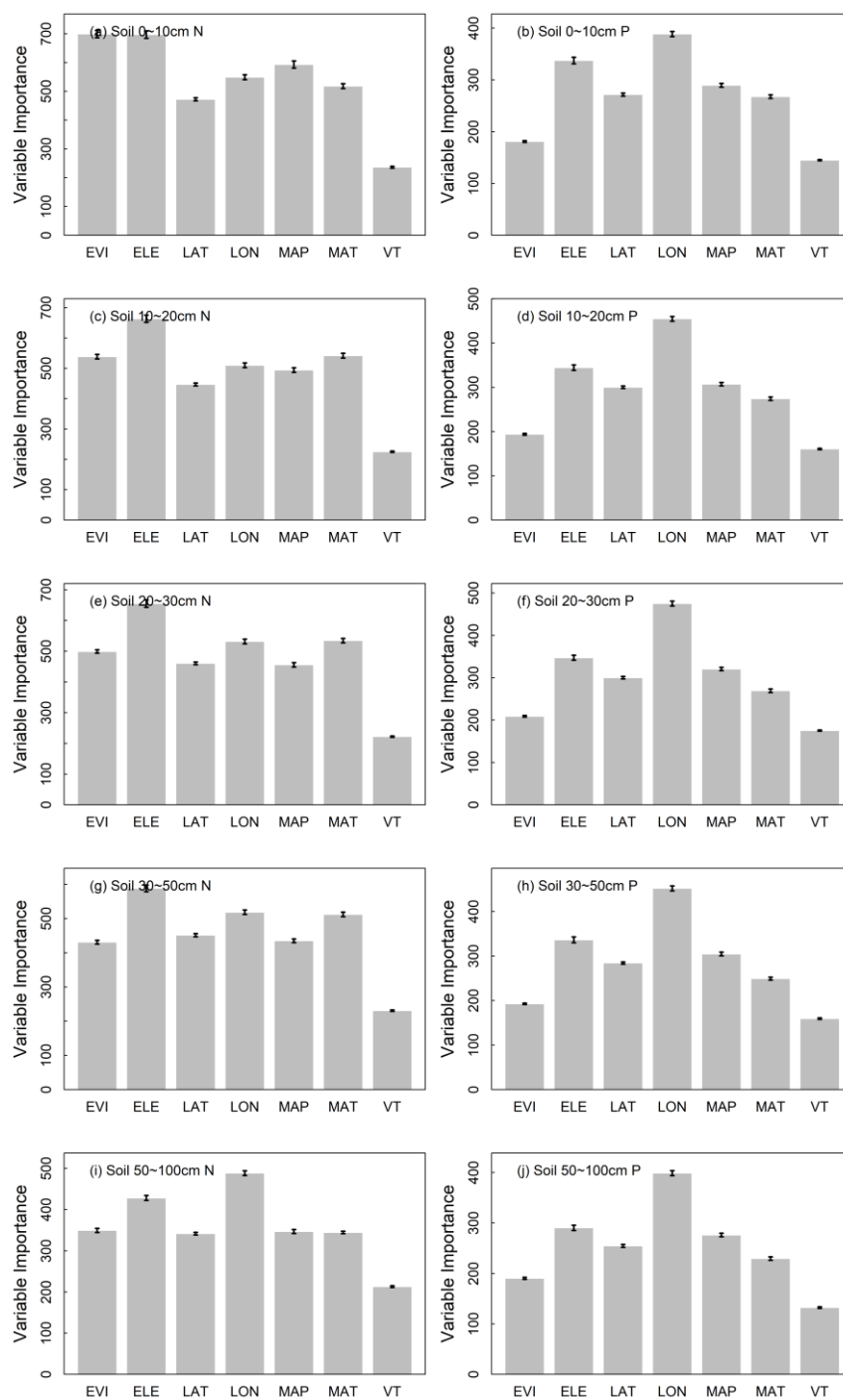


Fig. S11. The relative importance of variables in random forest models of N and P concentrations for 0-10 cm (a & b), 10-20 cm (c & d), 20-30 cm (e & f) 30-50 cm (g & h) and 50-100 cm (i & j) soil layers.